OLVASÓTERMI PÉLDÁNY TK 155.245

KFKI-1980-123

W. BAUHOFF
H.V. GERAMB
G. PÁLLA

STUDY OF NONLOCAL AND LOCAL EQUIVALENT MICROSCOPIC OPTICAL POTENTIALS

Hungarian Academy of Sciences

CENTRAL
RESEARCH
INSTITUTE FOR
PHYSICS

BUDAPEST

2017

KFKI-1980-123

STUDY OF NONLOCAL AND LOCAL EQUIVALENT MICROSCOPIC OPTICAL POTENTIALS

W. Bauhoff*, H.V. Geramb*, G. Pálla

Central Research Institute for Physics
H-1525 Budapest 114, P.O.B. 49, Hungary

*Theoretische Kernphysik, Univ. Hamburg
2000 Hamburg 50, Luruper Chaussee 149, W.-Germany

HU ISSN 0368 5330
ISBN 963 371 768 X

ABSTRACT

Medium energy elastic scattering is analysed with a microscopically generated nonlocal nucleon nucleus optical model and new features are delineated. A thourough discussion is presented in terms of exact phase equivalent local potentials that reveal a strong repulsive ℓ-dependent core which is beyond phenomenological potential models. The numerical part is limited to 40, 180, 200 MeV scattering from ^{12}C and 30, 180 MeV scattering from ^{40}Ca. Possible experiments to check the new features in angular distributions are discussed.

АННОТАЦИЯ

Упругое рассеяние нуклонов при средних энергиях исследовалось на основе микроскопического оптического потенциала, и было открыто новое специфическое явление. По анализу эквивалентного по фазе локального потенциала показано существование отталкивающего, зависящего от ℓ кора, не существующего в феноменологических моделях. Сделаны расчеты в случаях рассеяния протонов с энергией 40, 180 и 200 МэВ на ^{12}C и протонов с энергией 30 и 180 МэВ на ^{40}Ca. Обсуждается возможность экспериментального доказательства этого нового явления в измерении углового распределения протонов.

KIVONAT

Közepes energiáju rugalmas szórást vizsgáltunk mikroszkopikusan származtatott nukleon-mag optikai potenciál alapján és uj sajátságos jelenséget deritettünk fel. Ezen optikai potenciál diszkussziója során az exakt fázis equivalens lokális potenciál alapján kimutatunk egy taszitó, ℓ-függő törzs jelenlétét a potenciálban, amelyről a fenomenologikus modellek nem tudnak számot adni. A numerikus vizsgálatokat a ^{12}C-en való 40, 180 és 200 MeV-es szórásra, továbbá a ^{40}Ca-on való 30 és 180 MeV-es szórásra korlátoztuk. A feltárt uj jelenség szögeloszlásban való kisérleti igazolásának lehetőségét diszkutáljuk.

1. *Introduction*

The theoretical study of elastic scattering processes in nuclear physics is a fundamental step in understanding the nuclear many body problem. To its solution the last three decades have put forward various approaches, lying between purely phenomenological and fully microscopic. Nucleon nucleus scattering represents thereby the forefront to studies with more complex projectiles and we consider the derivation of a complex single particle potential, the optical model potential (OMP), from the elementary nucleon-nucleon interaction as ultimate goal [1]. The nuclear matter approach has itself established as a qualitative and quantitative method to reconcile the success of the phenomenological local optical model potentials with a purely microscopic model [2].

It lies in the nature of the microscopic theory that various approximations are used, of which some are model truncations and some are solely computational conveniences. With the latter approximations reference is made to solution techniques of the Bethe-Goldstone equation [2,3], computations of the nonlocal folded OMP with nuclear matter t-matrices, use of various forms for the diagonal and mixed single particle ground state density [4] and, what is of our concern, the transition from nonlocal to local equivalent potentials.

In this paper we resume to study problems and effects arising from the microscopic nonlocal OMP in differential cross section, and polarization data. Closely connected with this aim is a study of local equivalent potentials in order to disclose important shortcomings of phenomenological OMP's. With this remark we recall that for a nonlocal operator one cannot tell if the interaction is purely attractive or purely repulsive simply by knowing the over-all sign.

One must consider the detailed structure of the nonlocality and its behaviour as a function of energy and angular momentum. Some potentials behave attractive at low energy and repulsive at high energy. Similarly the behaviour may change for different angular momenta and thus result in an effective ℓ-dependent potential, here OMP.

The investigation of Perey and Buck [5] for neutron scattering below 25 MeV with the Frahn and Lemmer [6] type nonlocal potential is well known. The important result of this analysis was the reproduction of the energy dependence of local potentials with an energy-independent nonlocal potential and the reproduction of local phenomenological OMP as equivalent potentials. Furthermore, the transition from nonlocal potentials to equivalent local potentials was achieved with well working approximative analytic expressions which were little altered since [7].

It has been pointed out by Austern [8], later by Fiedeldey [9] and other authors [10] that nonlocal potentials are best elucidated by exact equivalent local potentials (LEQ) which are uniquely determined by a pair of linear independent solutions to the nonlocal problems. An essential ingredient in this formulation is the damping of the nonlocal wave function as compared to the local wave functions of the equivalent local potential. This effect, known as Perey effect [8,11], manifests an important difference between Schroedinger equations with a local and a nonlocal potential operator. A pair of linear independent solutions to local problems yields a Wronski determinant which is, independent of the radius, a constant. This radial independence of the Wronskian is generally not true for nonlocal potentials. Most of our results are built on this difference, which is a rigorous mathematical property. In other words, it makes it impossible to establish the full equivalence in phase and magnitude between local and nonlocal potential solutions without introducing singular potentials.

In section II we review the salient features of the microscopic nonlocal optical potential as it may be generated from nuclear matter t-matrices . This potential is understood as exemplaric mean of a microscopic theory and it may be substituted straight forward by other approaches [12,13].
Following the theoretical and mathematical background the definition of exact phase equivalent potentials in terms of nonlocal Wronskians and their derivatives is given.
Section III contains the formulation of the LEQ when replacing the nonlocal Wronskians and its derivatives by pure properties of the nonlocal potential. The final result of this section is a rapidly converging series expansion of LEQ. Several numerical examples are given to show qualitatively and quantitatively the differences to other methods to define equivalent local potentials. An application with quantitative results for 4o, 18o, 2oo MeV $^{12}C(p,p)$ and 16o,18o MeV $^{4o}Ca(p,p)$ are given in section IV. Withthis calculation we show the essential differences between phenomenological optical models and the microscopic optical potential as they manifest themselves at low and high energy. The essentials of this result shall be the occurence of a repulsive core in the LEQ whose radius increases with angular momentum.
As compared with phenomenological potentials this establishes the importance of nonlocal potential analyses for scattering above 1oo MeV. For lower energies we confirm that energy dependent and ℓ-independent potentials are sufficient to describe the global OMP. This is a numerical result irrespectively that the repulsive core exists as energy independent entity. Together with a comparison of 2oo MeV proton scattering data we discuss ℓ-dependent features in the angular distribution which should be experimentally verified. The latter statement is equivalent to postulate medium energy optical model analyses with nonlocal potentials.

2. *Theoretical background*

The study of interacting nucleons in infinitely extended nuclear matter is well established and approximate treatments for finite nuclei seem justified. Methods developed by Brückner and Bethe (BB) have thereby been widely applied and the theory with calculational procedures for the understanding of nucleon-nucleus elastic scattering starting from a realistic NN force is on from ground [1,2,3].
The approach pursued in our studies is based on the evaluation of the effective internucleon t-matrix from the free NN interaction [3]. The real and imaginary optical model for nucleons we calculate to first order in the effective NN interaction with an improved version of the local density approximation (LDA) in a folding approach with single particle target densities. The model relies on the quite general approach to generate in first approximation the OMP as a sum of a direct term and a non-local exchange term

$$U(\vec{r},\vec{r}';E) = \delta(\vec{r}-\vec{r}')\sum_n \int \phi_n^*(\vec{x})\; t_D(|\vec{r}-\vec{x}|;E)\,\phi_n(\vec{x})\,d^3x$$

$$+ \sum_n \phi_n^*(\vec{r})\, t_E(|\vec{r}-\vec{r}'|;E)\,\phi_n(\vec{r}') \qquad (1)$$

The coordinates $\vec{r}$ and $\vec{r}'$ refer to projectile coordinates. with the summation of single particle wave functions we represent the best possible (Hartree-Fock) particle densities - diagonal and mixed densities - for protons and neutrons. The basic ingredients of the LDA enters here in the choice of t_D and t_E which are mixtures of direct and exchange effective NN interactions [3].
In principle it should be calculated in the finite system with its full structural details. The
hypothesis is made that this effective interaction can be approximated by the one corresponding to the local density and energy dependent situation in nuclear matter. This effective interaction is our version of LDA.

The interaction contains automatically real and imaginary parts and the correct features of the finite range of the interaction. This is important since the ranges are different for real and imaginary parts and the relative spin and isospin channels. Any other approximation inherent in the nuclear matter approach in computing the effective interactions remains unaltered to previous calculations.

The stationary Schroedinger equation

$$\Delta\psi(\vec{r},\vec{k}) + (k^2-v_D)\psi(\vec{r},\vec{k}) = \int u(\vec{r},\vec{r}';E)\,\psi(\vec{r}',\vec{k})\,d\vec{r}' \qquad (2)$$

for the single particle OMP scattering solutions is most easily solved in the standard partial wave decomposition, where the numerical problem is reduced to an ordinary second order integrodifferential equation, viz.

$$\left[\frac{d^2}{dr^2} - \frac{L(L+1)}{r^2} + k^2 - v_D(r)\right] u_{LJ}(r) = \int_0^\infty \omega_L(r,r')\; u_{LJ}(r')\,dr' \qquad (3)$$

The diagonal potential v_D contains the standard homogenous charged sphere Coulomb potential and the spin orbit potential which we kept in a local form [3].
The multipole decomposition of the nonlocal OMP is formally obtained for a rotational invariant symmetric potential from

$$u(\vec{r},\vec{r}') = u_D(r)\,\delta(\vec{r}-\vec{r}') + u_E(\vec{r},\vec{r}')$$

$$= \sum_L \omega_L(r,r')_{/rr'}\,(Y_L(\hat{r})\cdot Y_L(\hat{r}')) \qquad (4)$$

$$= \sum_L \frac{(2L+1)}{4\pi}\,\omega_L(r,r')\;P_L(\hat{r}\cdot\hat{r}')_{/rr'}$$

The local direct potential is subsummized into the nonlocal knockout exchange potential which represents the proper source of nonlocality. The energy dependence in (1) results from the small energy dependence of the effective interaction. The multipole decomposition, eq. (4) is technically straight forward but is numerically quite involved due to required energy and density interpolation of numerically stored effective interactions.

The folding integral for the direct potential is simple and was generated with a Gauss-Legendre integration routine when performing the radial and angular integrations.

$$u_D(r) = 2\pi \int_0^\infty dr' \int_{-1}^{1} dx \sum_{lj,\tau} S_{lj}^{\tau} \phi^2_{lj,\tau}(\sqrt{r^2+r'^2+2rr'x}) \qquad (5)$$

$$t^D(r', k_F(r), E(r))$$

with S_{lj}^{τ} specifying the occupation number in the single particle orbit (lj) for protons/neutrons (τ). The radial wave functions $\phi_{lj,\tau}(r)$ are solutions of a Frahn-Lemmer type nonlocal bound state potential [14] with parameters V_o = - 72 MeV, R = 1,2 $A^{1/3}$ fm, a = o.65 fm, and the range of nonlocality β = o.8 fm. Coulomb and spin orbit potentials are kept in the standard local form with V_{ls} = 7 MeV, R_{ls} = 1.1 $A^{1/3}$ fm, a_{ls} = o.65 fm.
The exchange potential is best directly generated in its multipole decomposition

$$\sum_{ST,n} \psi_n(\vec{r})\psi_n(\vec{r}')\, t_E^{ST}(|\vec{r}-\vec{r}'|, k_F(\vec{r}+\vec{r}'/2), E(\vec{r}+\vec{r}'/2))$$

$$= \frac{1}{rr'} \sum \phi_{lj,\tau}(r)\phi_{lj,\tau}(r')\, t_E^{ST}(|\vec{r}-\vec{r}'|, k_F, E) \qquad (6)$$

$$y_{lj,m}(\hat{r})\, y^*_{lj,m}(\hat{r}')\, S_{lj}^{\tau}$$

In the limit of no-spin/isospinflip this expression assumes the form

$$\mathcal{U}_{EX}(\vec{r},\vec{r}') = \frac{1}{rr'} \sum \phi_{e_j,\tau}(r)\,\phi_{e_j,\tau}(r')\,S^{\tau}_{e_j} \langle \ell\, 1/2\, \mu\, \nu | j\, m\rangle^2$$

$$(-)^{S+T+1} \langle 1/2\, 1/2\, \nu\, \chi | S\, m_s\rangle^2 \langle 1/2\, 1/2\, \tau\, \varepsilon | T\, m_T\rangle^2 \qquad (7)$$

$$Y_{e\mu}(\hat{r})\, Y^{*}_{e\mu}(\hat{r}')\, t^{ST}(|\vec{r}-\vec{r}'|, k_F, E)$$

Together with a multipole expansion of the effective interaction

$$t^{ST}_{E}(|\vec{r}-\vec{r}'|, k_F, E) = \sum_{\lambda} t^{ST}_{\lambda}(r,r')\,(Y_{\lambda}(\hat{r})\cdot Y_{\lambda}(\hat{r}')) \qquad (8)$$

we obtain

$$\omega^{E}_{L}(r,r') = \sum_{\substack{lj,\tau \\ \lambda}} \phi_{lj,\tau}(r)\,\phi_{lj,\tau}(r')\langle l\lambda oo | Lo\rangle^2 \qquad (9)$$

$$S^{\tau}_{lj}\,\frac{\hat{\lambda}}{2\pi\,\hat{L}}\,\{\frac{1}{4}\,(t^{o1}_{\lambda} - 3\,t^{11}_{\lambda})\,\delta_{p,\tau} + \frac{1}{16}\,(3t^{1o}_{\lambda} + t^{o1}_{\lambda} - t^{oo}_{\lambda} - 3t^{11}_{\lambda})\,(1-\delta_{p\tau})$$

The isospin (proton/neutron) of the projectile enters through the index p (for projectile) on the Kronecker symbol $\delta_{p,\tau}$ and accounts for like or unlike projectile and target nucleons. As already mentioned, the required multipoles $t^{ST}_{\lambda}(r,r')$ are computed from tabulated values $t^{ST}(s,k_F,E)$. To eliminate possible errors in interpolations we apply a double transformation and obtain

$$t^{ST}_{\lambda}(r,r') = 8 \int_{o}^{\infty} k\,dk\; j_{\lambda}(kr)\,j_{\lambda}(kr') \int_{o}^{\infty} r\,dr\; \sin(kr)\,t^{ST}(|\vec{r}-\vec{r}'|) \qquad (10)$$

An impression of the nonlocal exchange kernel is obtained from Fig. 1 and 2 where the radial dependence $\omega^{E}_{o}(r,r')$ is shown for ^{40}Ca, 60 MeV with cuts across the diagonal r + r' = 6 fm and L = o(1)5. The multipole expansion of the local direct potential is straight forward and yields an L independent purely diagonal one:

$$\omega^{D}_{L}(r,r) = u_D(r)\,\delta(r-r') \qquad (11)$$

With the generation of the nonlocal kernel for the central real/imaginary potentials and the spin orbit potentials all ingredients of eq. (3) are available. It remains to solve the radial integrodifferential equation and extract the S-matrix elements in the usual matching procedure.
Spurious states or bound states in the continuum are known to exist for integrodifferential equations [15]. We defer further discussions to this problem since we checked our numerical results carefully and did not find any such case.

With this comment we may consider the problem solved and the comparison of theoretical predictions with experimental data can be done.

Since standard phenomenological OMP analysis uses local potentials it appears desireable to further delineate properties in the language of local potentials. We therefore outline the salient features of the transformation of a Schroedinger equation with a nonlocal potential eq. (3) to a Schroedinger equation with a local potential

$$\left[\frac{d^2}{dr^2} - \frac{L(L+1)}{r^2} + k^2 - v_D(r)\right] U_{LJ}(r) = V_{eq}(r) U_{LJ}(r) \qquad (12)$$

The local potential $V_{eq}(r)$ is said to be equivalent to the nonlocal kernel $\omega_L(r,r')$ if it can be completely specified in terms of eq.(3) and its solutions and if it analytically reproduces observable features as a function of energy.
The transformation for the nonlocal equation requires two linear independent solutions with asymptotically unique boundary conditions for incoming and outcoming waves [9,10].
Boundary conditons in the interaction region may depend on the assumptions about the interaction which are not subject to direct observation. The asymptotic properties are maintained in the transformation and are the same for both eqs. (3) and (12).

These specifications and the analytic properties of any two linear independent solutions define the problem uniquely. Let $f_{1,2}(k,r)$ be two solutions to the nonlocal radial equation and $F_{1,2}(k,r)$ the equivalent solutions to the local equation. Both solutions satisfy the asymptotic boundary conditions

$$\lim_{r\to\infty} (f_i(k,r) - F_i(k,r)) = o \tag{13}$$

In the residual radial range we relate the solutions by a damping function

$$f_i(k,r) = A(k,r)\ F_i(k,r) \tag{14}$$

which behaves asymptotically

$$\lim_{r\to\infty} A(k,r) = 1 \tag{15}$$

This ansatz was first suggested by Austern [8] and it is intriguing as it depicts so many relevant physical quantities and yields a smooth regular equivalent local potential.
Any two linear independent solutions satisfy the Wronskian relation

$$W(f_1,f_2) = f_1(r)\ f_2'(r) - f_2(r)\ f_1'(r) \tag{16}$$

This Wronskian shows the essential difference between local and nonlocal Schroedinger equations. Eq. (16) is generally a function of the radius and stands as such contrary to the property of $W(F_1,F_2)$, the local Wronskian, which is radially independent for a regular potential. Ansatz (14) together with (15) relates the Wronskian

$$W(f_1,f_2) = A^2\ W(F_1,F_2) = W(F_1,F_2)\big|_{r=\infty} \tag{17}$$

by the damping functions. The damping function is in other literature often identified as Perey effect [8,11].

$$A(k,r) = \sqrt{W(f_1(k,r),\ f_2(k,r))/W(f_1(k,\infty),\ f_2(k,\infty))} \tag{18}$$

For symmetric kernels $\omega_L(r,r') = \omega_L(r',r)$

$\lim_{r\to o} A(r) = 1$ and $\lim_{r\to o} W'(r) = o$

The equivalent local potential is constructed in the same manner [9,1o]. Combining eqs. (3) and (12) we may eliminate any reference to a particular pair of solutions and find by pure algebraic manipulations that

$$\begin{aligned} V_{eq}^{(2)}(r) &= -\frac{1}{2}\frac{W''(f_1,f_2)}{W(f_1,f_2)} + \frac{3}{4}\left(\frac{W'(f_1,f_2)}{W(f_1,f_2)}\right) \\ &\quad + \frac{1}{W(f_1,f_2)} \cdot \int_o^\infty \omega_L(r,r')\left[f_1(r')f_2'(r) - f_1'(r)f_2(r')\right]dr' \\ &= -\frac{A''}{A} + 2\left(\frac{A'}{A}\right)^2 + \frac{1}{A^2}\int_o^\infty \omega_L(r,r')\left[f_1(r')f_2'(r)\right. \\ &\quad \left. - f_2(r')f_1'(r)\right]dr' \end{aligned} \tag{19}$$

The expression for the damping functions and equivalent local potentials provides a unique and mathematically rigorous definition of these ℓ-dependent quantities throughout the domain of existence of solutions to the nonlocal equation. Herewith we have a mean to compare properties of microscopic ℓ-dependent potentials with phenomenological potentials working.

3. *Analytic representation of the local ℓ-dependent potentials.*

Though eq. (19) gives an exact expression for the local equivalent potential, it is quite cumbersome to be used in practice since two independent solutions are needed for the calculation. Therefore, it seems desirable to develop an approximation scheme for the calculation of $V_{eq}(r)$. The quality of the approximation can then be tested by comparison with the exact formula (19). Such a comparison was not possible for other approximations used so far because they did not make use of an angular momentum decomposition. The basic idea of the approximation scheme is to use an perturbation expansion with respect to the nonlocality range of the integral kernel. It is a simple exercise to prove the following equality for any symmetric integral kernel $\omega(r,r')$:

$$\omega(r,r') = \sum_{n=o}^{\infty} \frac{(-1)^n}{n!} e^{ik_o(r-r')} \delta^{(n)}(r-r') \; v_n\left(\frac{r+r'}{2}; k_o\right) \qquad (2o)$$

where $k_o = k_o(\frac{r+r'}{2})$ is an arbitrary function to be chosen later. The expansion coefficients $v_n(R;k_o)$ are determined by the following equation:

$$v_n(R;k_o) = \int_{-2R}^{2R} e^{-ik_o s} \, s^n \omega(R - \tfrac{1}{2}s, \; R + \tfrac{1}{2}s)\, ds \qquad (21)$$

So they are the n-th moments of the integral kernel $\omega(r,r')$. The approximation scheme to be described may be called momentum expansion. For the special case $k_o(R) \equiv o$ this type of expansion has been used in the framework of generator coordinate theory [16]. Since in our case the arguments of $\omega(r,r')$ are restricted to positive values the integration with respect to $s = r-r'$ is on a finite interval only.

It is now important to note that the moments $v_n(R;k_o)$ will decrease rather rapidly with increasing n due to the peculiar form of the integral kernel. Since $\omega(r,r')$ is strongly peaked at $s = r - r' = o$, an appreciable contribution to the integral (21) may come from the region of small s. The factor s^n, however, is small there for $n > o$, so the value of the whole integral will

decrease with increasing n. From this consideration, it is suggestive to consider (2o) as a perturbation expansion of the integral kernel. To emphasize this idea, a parameter λ will be introduced to characterize the magnitude of the various orders so that eq. (2o) can be written:

$$\omega(r,r') = \sum_{n=o}^{\infty} \lambda^n V_n(r,r';k_o) \tag{22a}$$

with

$$V_n(r,r';k_o) = \frac{(-1)^n}{n!} e^{ik_o(r-r')} \delta^{(n)}(r-r') v_n(\frac{r+r'}{2};k_o) \tag{22b}$$

If this expansion is introduced into the nonlocal Schroedinger equation, a corresponding expansion for the wave-function is appropriate:

$$f(r) = \sum_n \lambda^n \psi_n(r) \tag{23}$$

Equating now equal powers of λ on both sides, the nonlocal Schroedinger equation is transformed into a set of local equations. The lowest order equations read explicitly:

$$\begin{aligned}
&\{\frac{d^2}{dr^2} - \frac{l(l-1)}{r^2} + k^2 - v_o(r)\}\psi_o(r) = o \\
&\{\frac{d^2}{dr^2} - \frac{l(l+1)}{r^2} + k^2 - v_o(r)\}\psi_1(r) = \int V_1(r,r'"k_o)\psi_o(r')dr' \\
&\{\frac{d^2}{dr^2} - \frac{l(l+1)}{r^2} + k^2 - v_o(r)\}\psi_2(r) = \int V_1(r,r';k_o)\psi_1(r')dr' \\
&\qquad\qquad + \int V_2(r,r';k_o)\psi_o(r')dr'
\end{aligned} \tag{24}$$

So the zeroth order equation is a usual local Schroedinger equation whereas all higher equations contain an inhomogeneous term, which is determined by the solution of the lower equations.

The first term on the r.h.s. vanishes due to eq. (26). Up to order λ we have:

$$\frac{W'(r)}{W(r)} = \frac{W_1'(r)}{W_o(\infty)} \tag{28}$$

With the definition (25) we find for the derivative:

$$W_1'(r) = \psi_o''(r)\varphi_1(r) + \psi_1''(r)\varphi_o(r) - \psi_o(r)\varphi_1''(r) - \psi_1(r)\varphi_o''(r) \tag{29}$$

The second derivatives of the wave-functions may now be eliminated with help of the Schroedinger equations (24). Many terms cancel, and it remains

$$\begin{aligned} W'(r) &= \varphi_o(r)\int V_1(r,r';k_o)\psi_o(r')\,dr' \\ &\quad - \psi_o(r)\int V_1(r,r';k_o)\varphi_o(r')\,dr' \end{aligned} \tag{30}$$

Finally, we use the definition (22b) for $V_1(r,r';k_o)$ to obtain

$$W_1'(r) = v_1(r;k_o)\left[\varphi_o(r)\psi_o'(r) - \varphi_o'(r)\psi_o(r)\right] \tag{31}$$

The expression in square brackets is $W_o(r) = W_o(\infty)$. $W_o(\infty)$ cancels in eq. (28) and we get as contribution to the potential $V_{eq}(r)$ from the term $\left(\frac{W'(r)}{W(r)}\right)^2$ up to order λ^2:

$$\left(\frac{W'(r)}{W(r)}\right)^2 = \lambda^2\, v_1^2(r;k_o) \tag{32}$$

As claimed at the beginning, this expression does not contain the wave-function anymore, but only the (first) moment of the integral kernel. Similarly, all other contributions to the phase equivalent potential can be calculated. The final result up to order λ^2 reads:

$$V_{eq}(r) = v_o(r;k_o) + \lambda\{-ik_o\, v_1(r;k_o)\}$$

$$+ \lambda^2\{\frac{1}{4}\, v_1^2(r;k_o) - \frac{1}{4}\, v_2''(r;k_o) + v_2(r;k_o) \qquad (33)$$

$$[\frac{l(l+1)}{r^2} - k^2 + v_o(r;k_o) - k_o^2]\}$$

Of course, $\lambda = 1$ in the final expression. The inclusion of higher order terms does not present principal difficulties but the calculations become rather lengthy.
If the whole series is summed, the result will not depend on the choice of $k_o(r)$. It is, however, important to choose it in an appropriate manner, if only a few terms are taken into account. By comparing the exact potential eq. (19) with the partial sum of the moment expansion it is possible to see whether the particular choice of $k_o(r)$ is a good one or not. It turns out that the agreement between exact potential and the zeroth order of the moment expansion is closest when $k_o(r)$ is chosen self-consistently [7] as the local momentum of the projectile

$$k_o^2(r) = k^2 - \frac{l(l+1)}{r^2} + v_o(r;k_o) \qquad (34)$$

All results presented in the following are obtained with this special $k_o(r)$. Also, only the zeroth order of the moment expansion is considered because it will be shown to be accurately enough.
In order to compare the various approaches for a phase equivalent local potential we consider first a model of a simple analytic form, the so-called Frahn-Lemmer [6] or Perey-Buck [5] potential, which is given by

$$u(\vec{r},\vec{r}') = \frac{V_o}{\gamma^3 \pi^{3/2}}\; e^{-(\vec{r}-\vec{r}')^2/\gamma^2} \left[1+e^{\frac{1}{a}(\frac{r+r'}{2} - R)}\right]^{-1} \qquad (35)$$

As $V_n(r,r';k_o)$ contains derivatives of the δ-function, the inhomogeneties are in fact local expressions containing derivatives of the wave functions. Second and higher derivatives of them may be eliminated by using the lower order equations. The two independent solutions $\psi(r)$, $\varphi(r)$ are expanded in the form (23), a corresponding expansion will result also for the Wronskian $W(r)$ which reads explicitly up to order λ

$$\begin{aligned} W(r) &= W_o(r) + \lambda W_1(r) + \ldots \\ &= [\psi_o(r)\varphi_o'(r) - \psi_o'(r)\varphi_o(r)] \\ &+ \lambda[\psi_o(r)\varphi_1'(r) + \psi_1(r)\varphi_o'(r) - \psi_o'(r)\varphi_1(r) - \psi_1'(r)\varphi_o(r)] \\ &+ \ldots \end{aligned} \tag{25}$$

From the set of equations (24) it is, however, seen that $W_o(r)$ is a Wronskian corresponding to a usual local Schroedinger equation. It is well-known that in this case the Wronskian does not depend on the radius,so we have the important result:

$$W_o(r) = W_o(\infty) = \text{const.} \tag{26}$$

After these preliminaries we return to the question of approximating the phase equivalent potential $V_{eq}(r)$, eq. (19). From the expansion in powers of λ for the integral kernel and the Wronskian we will get also an expansion for $V_{eq}(r)$. It will be shown that the various contributions can be calculated from the knowledge of the moments of the integral kernel and that any wave-function drops out of the final formula. The full calculation is rather lengthy, so we will consider only a single term to demonstrate the method. As an example take the term $(\frac{W'(r)}{W(r)})^2$. From (25) we have

$$W'(r) = W_o'(r) + \lambda W_1'(r) + \ldots \tag{27}$$

Its various multipole components can be calculated analytically [5]. The parameters have been chosen for ^{40}Ca i.e. R = 4.1 fm, a = o.65 fm. The depth was taken as V_o = - 72 MeV and the non-locality range was γ = o.8 fm. Various forms of the equivalent local potential [5] are shown in Fig. 3 for the s-wave at a projectile energy of 3o MeV. First of all, the trivial equivalent potential has so many singularities that a smooth interpolation is rather arbitrary. The exact phase-equivalent potential eq. (19) has a conventional Woods-Saxon shape at larger radii, but deviates from this form strongly at small distances. For r -> o it is even repulsive. The potential resulting from the moment expansion deviates only slightly from this form: it does not show the dip around 1 fm, and it vanishes at the origin. For comparison, also the usual Perey-Buck approximation is shown which does not depend on the angular momentum. It coincides with the moment expansion everywhere except close to the origin where it assumes a finite value.

In Fig. 4, we consider the energy dependence of the local potential resulting from the moment expansion. The behaviour at short distances is found to be independent of the energy whereas for larger distances the potential decreases almost linearly with the energy. The behaviour for different angular momenta at the same energy, shown in Fig. 5, is complementary to this: For large distances, the potential does not depend on l, whereas the short-distance is completely different for different angular momenta: The potential can be shown to start like r^{2l+3}.

The corresponding results for the real part of the microscopic optical potential are shown in Fig. 6 to 8. In this case one has to add a local (repulsive) potential to the nonlocal attractive one. Therefore, the behaviour close to the origin is dominated by the direct term which leads to the existence of a repulsive core. The various equivalent local potentials are compared in Fig. 6. The trivial equivalent potential does not have singularities because the wave function is now complex. Instead it shows finite jumps at the zeroes of the real part of the wave function. The exact potential has various oscillations for small distances which are interpolated by the moment expansion.

Such a behaviour had to be expected since the zeroth order is essentially given by a Wigner transform which cannot reproduce all quantum fluctuations. The local momentum approximation used by Brieva and Rook [3] is seen to defer strongly for all radii, so this approximation seems to be questionable.

The energy dependence of the local potential Fig. 7 is similar to that obtained for the Frahn-Lemmer potential. Much more interesting is the angular momentum dependence shown in Fig. 8. One observes the existence of a pronounced oscillation between 1 and 2 fm which is amplified for larger angular momenta.

For completeness we add in Figs. 9a to 9c the numerical results for the imaginary and spin orbit potentials together with the damping function for L = o. In fact, all these quantities are ℓ-dependent. We defer its representation due to its minor importance or little physical significance in interpreting results.

4. *Applications*

Microscopic optical potentials have proven to reproduce the global features of phenomenological results. To these features we count the energy dependence of volume integrals of real and imaginary central potentials, the rms radii and in some cases with adjustments of the strength by 1o-2o% the reproduction of differential cross sections and analyzing power data. With the here presented analysis we do not expect to achieve better fits but rather indicate characteristic which are inherent in nonlocal potentials.

The energy dependence of (equivalent) local potentials is well known as well as the damping of nonlocal wave functions. The success of Saxon-Woods potentials below 8o MeV on the other hand indicate that the inner region of the target nucleus does not enter sensitively in angular distributions. Inclusion of the ℓ-dependent core, as shown in previous sections, must therefore leave theoretical angular distribution unaltered. In Fig. 1o proton scattering from ^{12}C is displayed for 4o and 18o MeV. The angular distributions are calculated with the full phase equivalent microscopic OMP (LEQ MOP) Fig. 11 and 12 with/without spin orbit potentials (U_{So} = o). The second group of curves are obtained when the potential was replaced by the microscopic potential for l=o and its core eliminated. (LEQMOP without core). The results prove the importance of the core for high energies and being there comparable with the spin orbit effects. In Fig. 13 and 14 we compare the results with experimental data. Since LEQ MOP represents an ab initio calculation, parameterfree, its fit is excellent also when considering phenomenological fits. The 2oo MeV data give reason to believe that large angle scattering is most strongly influenced by the core. The minimum in $\sigma(\theta)$ around 95^o is followed by a back rise. Similar results are obtained for 16o, 18o MeV scattering from ^{4o}Ca, Figs. 15 - 1C. Again we emphasize the backrise after the minimum around 98^o. The forward region is well reproduced with a strongly damped diffraction pattern between 3o and 7o degrees.

In phenomenological analyses this damping was explained as a pure spin orbit effect. We interpret it rather as a mutual effect of the effective ℓ-dependent core and spin orbit potential. In view of the underlying "1o% theory" it is not our intention to overestimate the predictive power of microscopic OMP and their fits. On save ground is the backangle rise of the differential cross section. We interpret this as the essential feature of nonlocal potentials which produce strong trapping effects resulting in scattering paths into the backward region. In the language of LEQ MOP, we see radial region of rapidly varying attraction / repulsion. It remains as an experimental challenge to measure complete angular distributions with 2oo MeV projectile beyound 9o degrees for a few nuclei. Furthermore the analyses of future high energy data is proposed to be performed with nonlocal potentials which are fully microscopic or at least guided by it. Technically the phenomenological Frahn-Lemmer ansatz is convenient to handle in its multipole decomposition and it contains less free parameters as superpositions of several Saxon-Woods potentials.

References

1) Microscopic Optical Model Potential, ed. H.V. Geramb
Lecture Notes in Physics, Vol. 89, Springer 1979

2) J.P. Jeukenne, A. Lejeune and C. Mahaux
Phys. Reports 25C, (1976) 83

3) F.A. Brieva and J.R. Rook
Nucl. Phys. A291, (1977) 299, Nucl. Phys. A291, (1977) 317
Nucl. Phys. A297, (1978) 2o6

4) J.W. Negele and D. Vautherin, Phys. Rev. C5 (1972) 1472;
Phys. Rev. C11, (1975) 1o31
X. Campi and A. Bouyssy, Phys. Lett. 73B, (1978) 263
A. Tielens, Diplomarbeit, Hamburg 1979

5) F.G. Perey and B. Buck
Nucl. Phys. 32, (1962) 353

6) W.E. Frahn and R.H. Lemmer
Nuovo Cim. 5, (1957) 523; Nuovo Cim. 6, (1957) 664

7) F.G. Perey and D.S. Saxon, Phys. Lett. 1o, (1964) 1o7
W.E. Frahn, Nucl. Phys. 66, (1965) 358
R. Peierls and N. Vinh Mau, Nucl. Phys. A343, (198o) 1
H. Horiuchi, Progr. Theor. Phys. 64, (198o) 184

8) N. Austern
Phys. Rev. 137, (1965) B752

9) H. Fiedeldey
Nucl. Phys. 77, (1966) 149
Nucl. Phys. A96, (1967) 463
Nucl. Phys. A115, (1968) 97

1o) M. Coz, R.G. Arnold and A.D. MacKellar
Ann. Phys. 58, (197o) 5o4, Ann. Phys. 59, (197o) 219

11) F.G. Perey
Direct Interactions and Nuclear Reaction Mechanisms
(E. Clement, C. Villi, eds.) Gordon and Breach (1958) p 125

12) N. Vinh Mau and A. Bouyssy
Nucl. Phys. A257, (1976) 189

13) M.K. Weigel and G. Wegmann
Fortschritte d. Phys. 19, (1971) 451

14) T. Ueberall
Diplomarbeit Hamburg (1979)

15) L.G. Arnold and A.D. MacKellar
Phys. Rev. C3, (1971) 1095
Th. O. Krause, M. Mulligan
Ann. Phys. 94, (1975) 31
B. Mulligan, L.G. Arnold, B. Badchi and T.O. Krause
Phys. Rev. C13, (1976) 2131

16) B. Giroud and B. Grammaticos
Ann. Phys. 101, (1976) 670

17) B.W. Riedley and J.F. Turner
Nucl. Phys. 58, (1964) 497

18) H.O. Meyer, P. Schwandt, G.L. Moake and P.P. Singh
IUCF (1980) 385

19) A. Nadasen, P. Schwandt, P.P. Singh, W.W. Jacobs,
A.D. Bacher, P.T. Debecev, M.D. Kaitchuck and J.T. Meek
IUCF (1979) 118

Figure Captions

Fig. 1 Triaxial representation of the real nonlocal exchange kernel $\omega_o^E(r,r')$. The underlying geometry is ^{4o}Ca for 6o MeV.

Fig. 2 Cuts of nonlocal exchange kernels $\omega_L^E(r,r')$ real - solid lines, imaginary - dashed lines for various angular momenta.

Fig. 3 Comparison of equivalent local potentials, generated within different prescriptions. The Wronski method (solid line) is the exact result for eq. (19) and moment expansion refers to eq. (33). Perey Buck and trivial equivalent potential coincide with its definition in ref. 5.

Fig. 4 Energy dependence of the local equivalent Frahn-Lemmer typ potential generated with moment expansion.

Fig. 5 Study of the ℓ-dependence L = o,1...2o of the equivalent Frahn-Lemmer potential for 3o MeV nucleons.

Fig. 6 Comparison of various equivalent local potential prescriptions when applied to the full microscopic optical model kernel. Wronski refers to the exact solution of eq. (19) and moment expansion to the application of eq. (33). Local momentum approximation refers to the prescription used in ref. 3. Trivial equivalent is identical with ref. 5.

Fig. 7 Study of the energy dependence of LEQ within the moment expansion.

Fig. 8a ℓ-pedendence of the real part of LEQ within the moment expansion.

Fig. 8b ℓ-dependence of the imaginary part of LEQ within the moment expansion

Fig. 9a Study of the energy dependence of full imaginary central potential.

Fig. 9b Local spin orbit potentials generated with expressions developed in ref. 3.

Fig. 9c Energy dependence of the real part of the damping function (Perey effect) for L = o based on the full nonlocal kernel. The damping functions are ℓ-dependent and change visually like the potentials shown in fig. 5.

Fig. 1o Effects of the repulsive ℓ-dependent core on differential cross sections at low and high energy. The geometrical ingredients are from ^{12}C.

Fig. 11a 4o MeV ℓ-dependent real central potentials underlying the calculations in fig. 1o.

Fig. 11b 4o MeV ℓ-dependent imaginary central potentials underlying the calculations in fig. 1o

Fig. 12a 18o MeV ℓ-dependent real central potentials underlying the calculations in fig. 1o.

Fig. 12b 18o MeV ℓ-dependent imaginary central potentials underlying the calculations in fig. 1o.

Fig. 13 ^{12}C proton scattering analyses for two energies. The data are from literature [17,18]. Phenomenological OMP 1 and 2 are the best fit potentials of ref. 18 which apply single and double Saxon-Woods form factors in their fit procedures.

Fig. 14 Polarisations to the 2oo MeV analyses in fig. 13.

Fig. 15a Comparison of 16o MeV proton experiment with theoretical prediction with the LEQ. Data from ref. 19.

Fig. 15b Comparison of 18o MeV proton experiment with theoretical prediction with the LEQ. Data from ref. 19.

Fig. 16a 18o MeV ℓ-dependent real central potential underlying the calculations in fig. 15ℓ.

Fig. 16b 18o MeV ℓ-dependent imaginary central potential underlying the calculations in fig. 15ℓ.

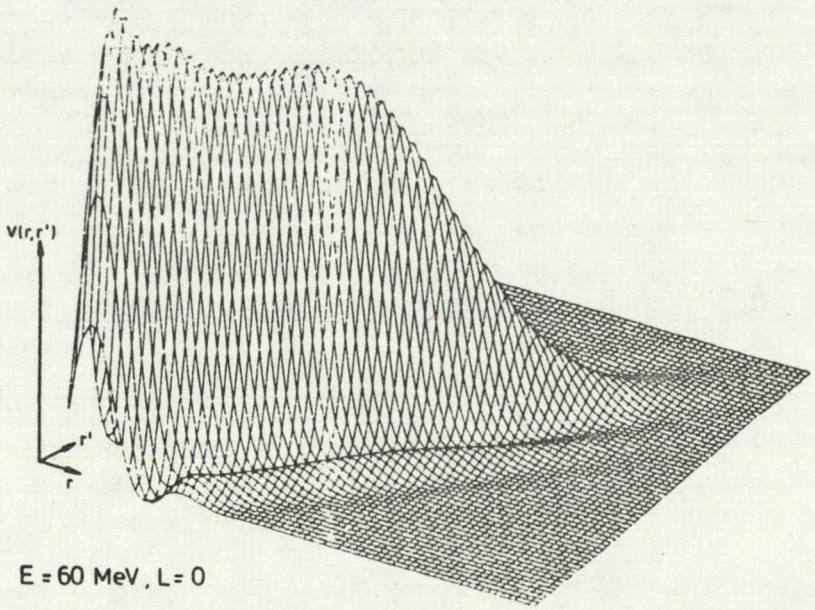

FIG. 1

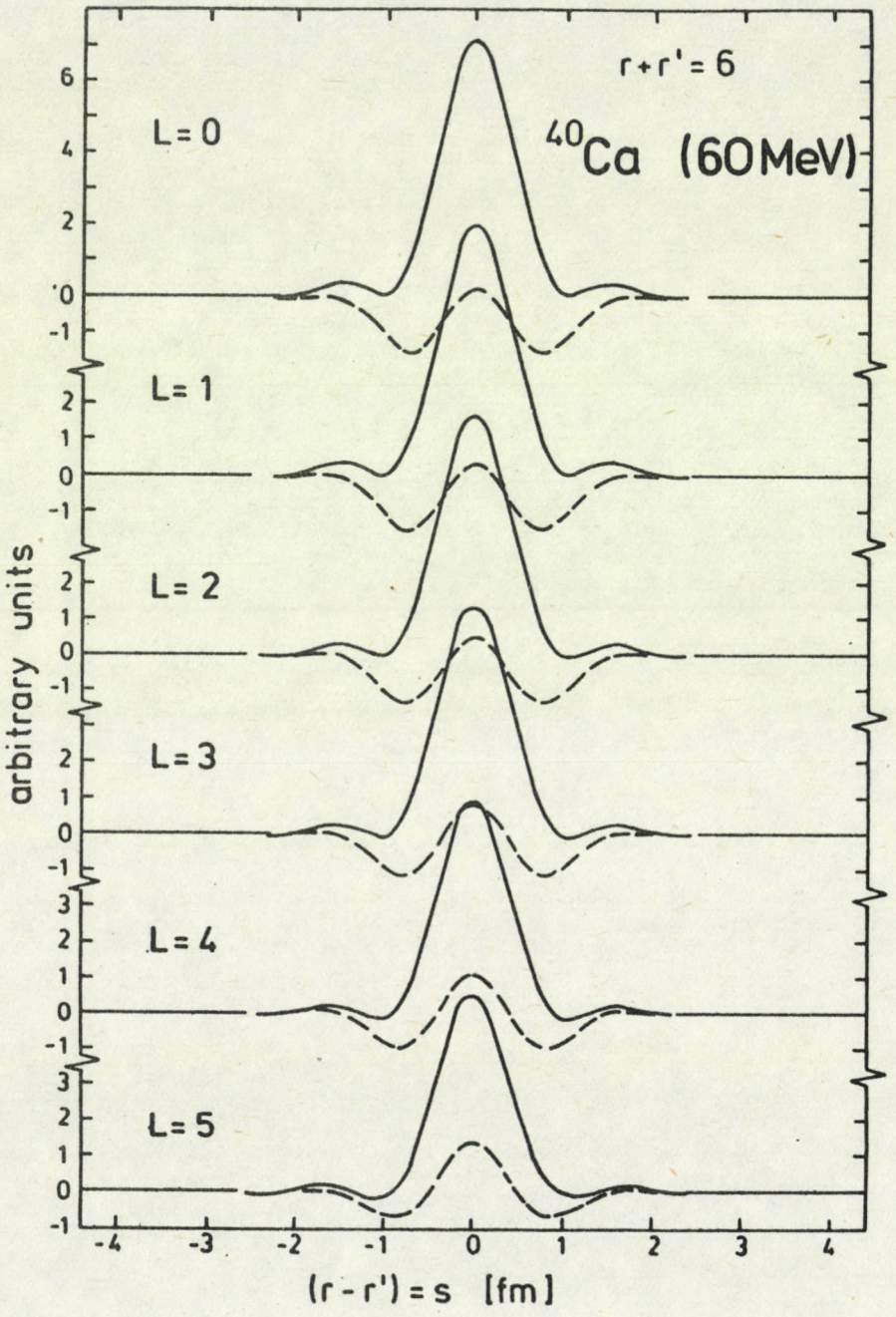

FIG. 2

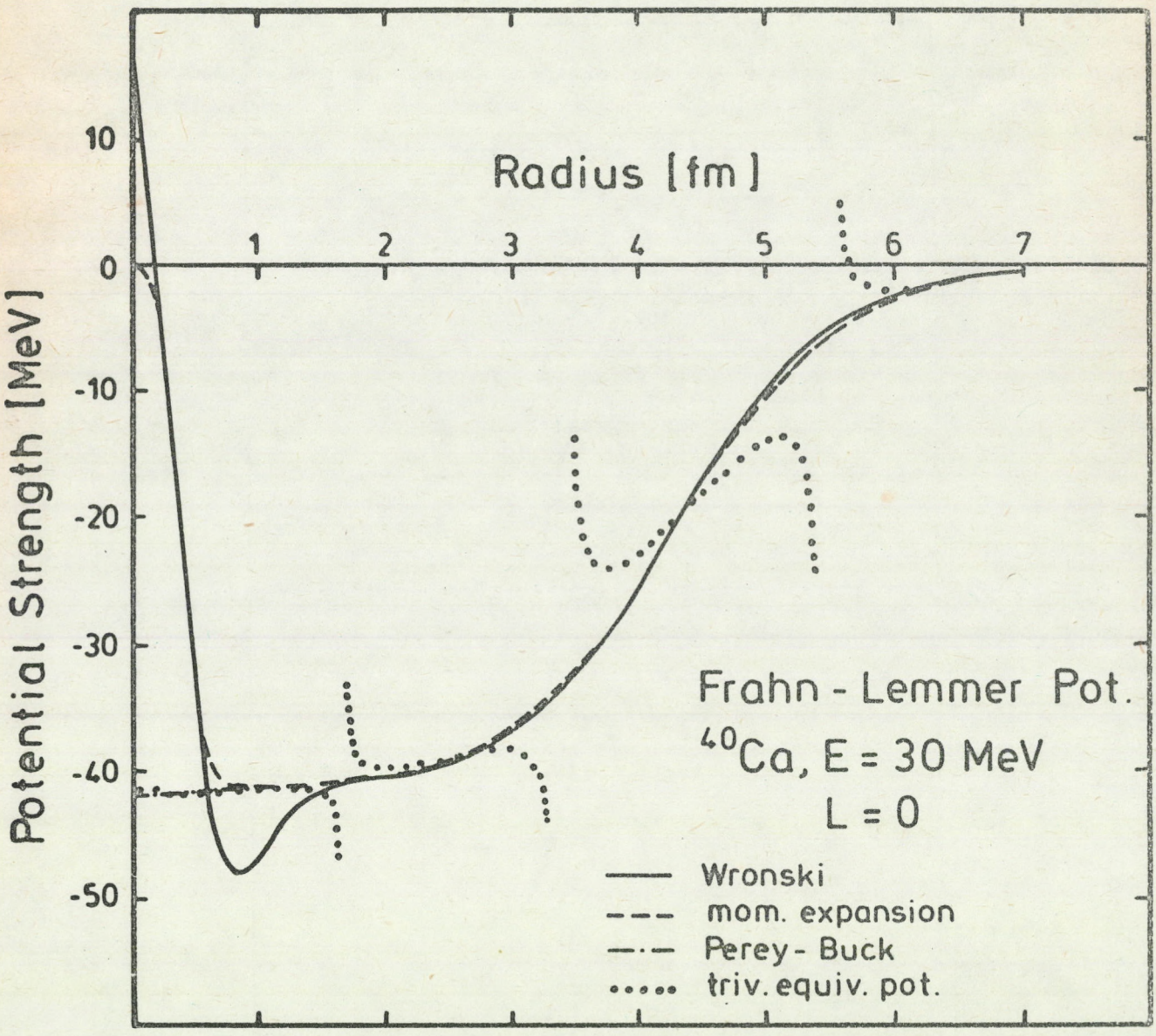
Radius [fm]
1
2
3
4
5
6
7
10
0
-10
-20
-30
-40
-50
Potential Strength [MeV]
Frahn - Lemmer Pot.
40Ca, E = 30 MeV
L = 0
Wronski
mom. expansion
Perey - Buck
triv. equiv. pot.

FIG. 3

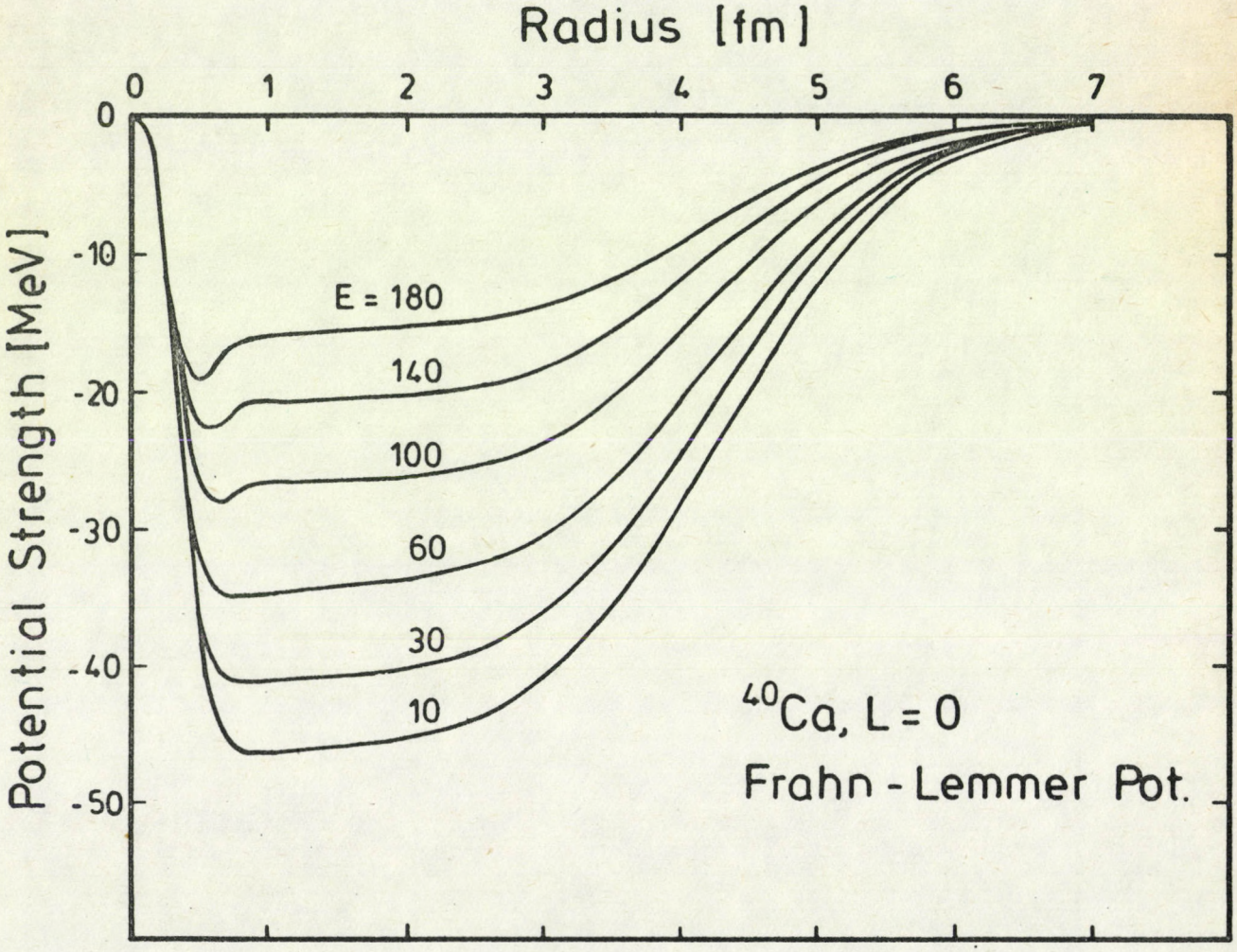
Radius [fm]
0
1
2
3
4
5
6
7
Potential Strength [MeV]
0
-10
-20
-30
-40
-50
E = 180
140
100
60
30
10
40Ca, L = 0
Frahn - Lemmer Pot.

FIG. 4

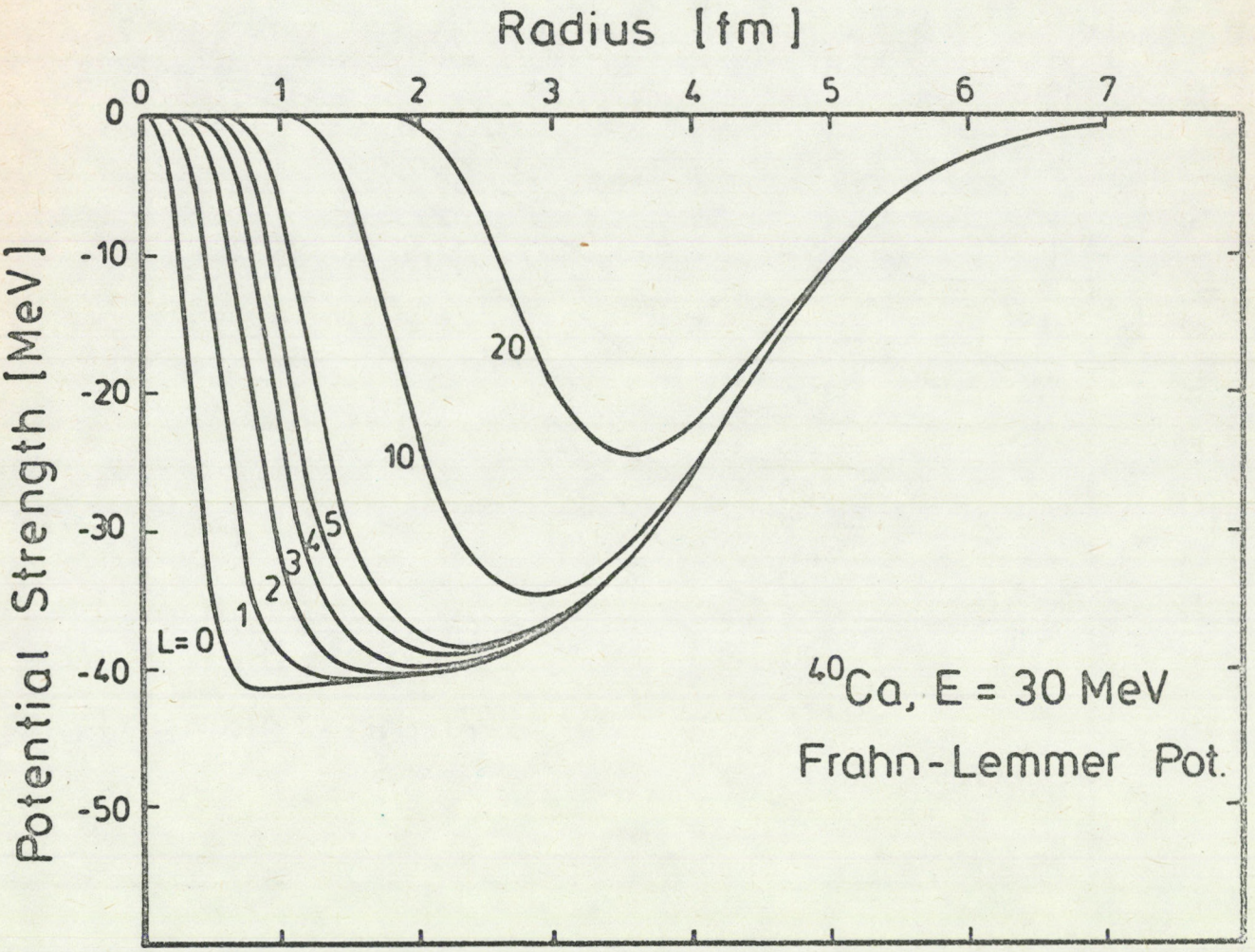
Radius [fm]
0
1
2
3
4
5
6
7
Potential Strength [MeV]
0
-10
-20
-30
-40
-50
L=0
1
2
3
4
5
10
20
40Ca, E = 30 MeV
Frahn-Lemmer Pot.

FIG. 5

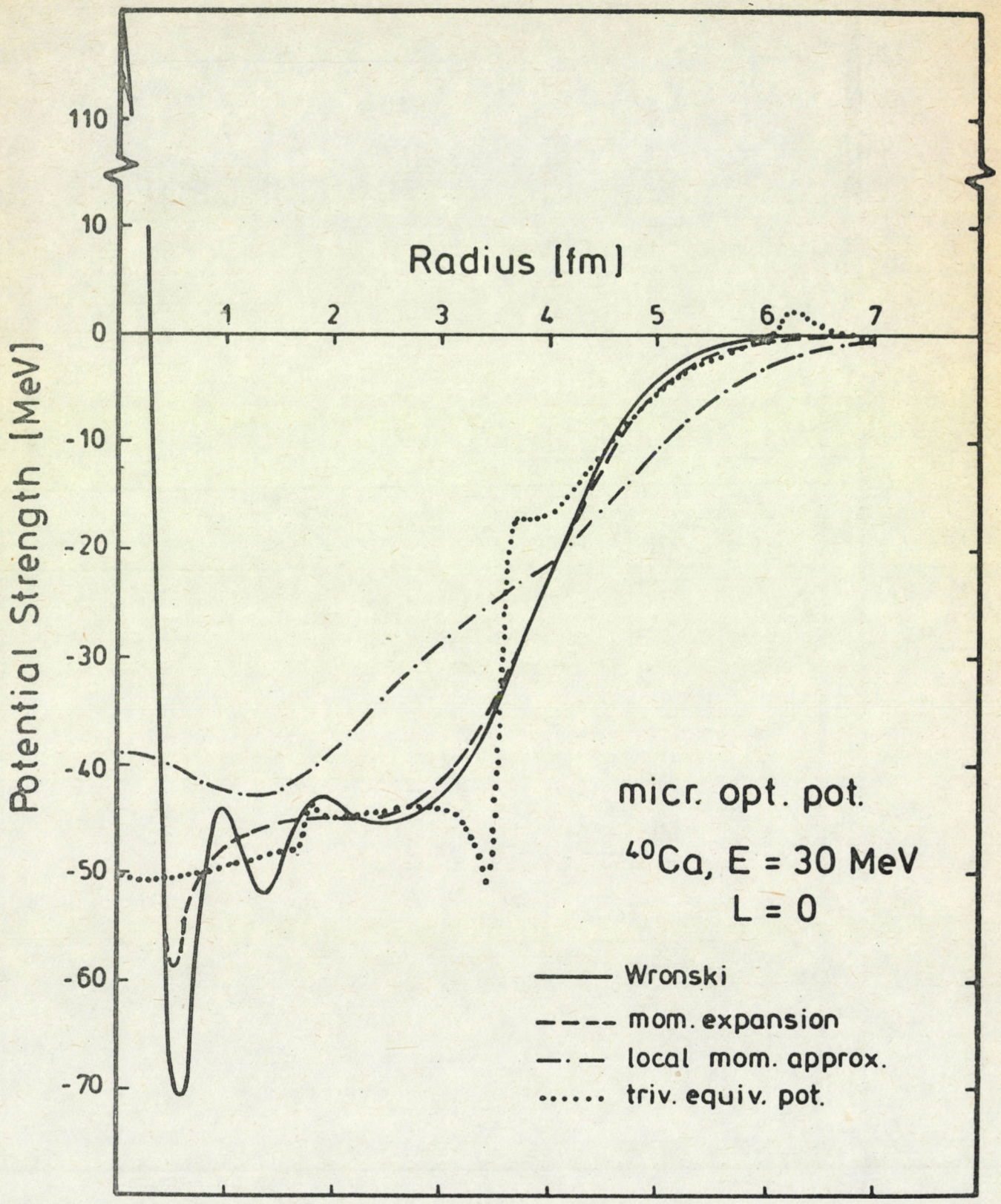
Radius [fm]
Potential Strength [MeV]
110
10
0
-10
-20
-30
-40
-50
-60
-70
1
2
3
4
5
6
7
micr. opt. pot.
40Ca, E = 30 MeV
L = 0
Wronski
mom. expansion
local mom. approx.
triv. equiv. pot.

FIG. 6

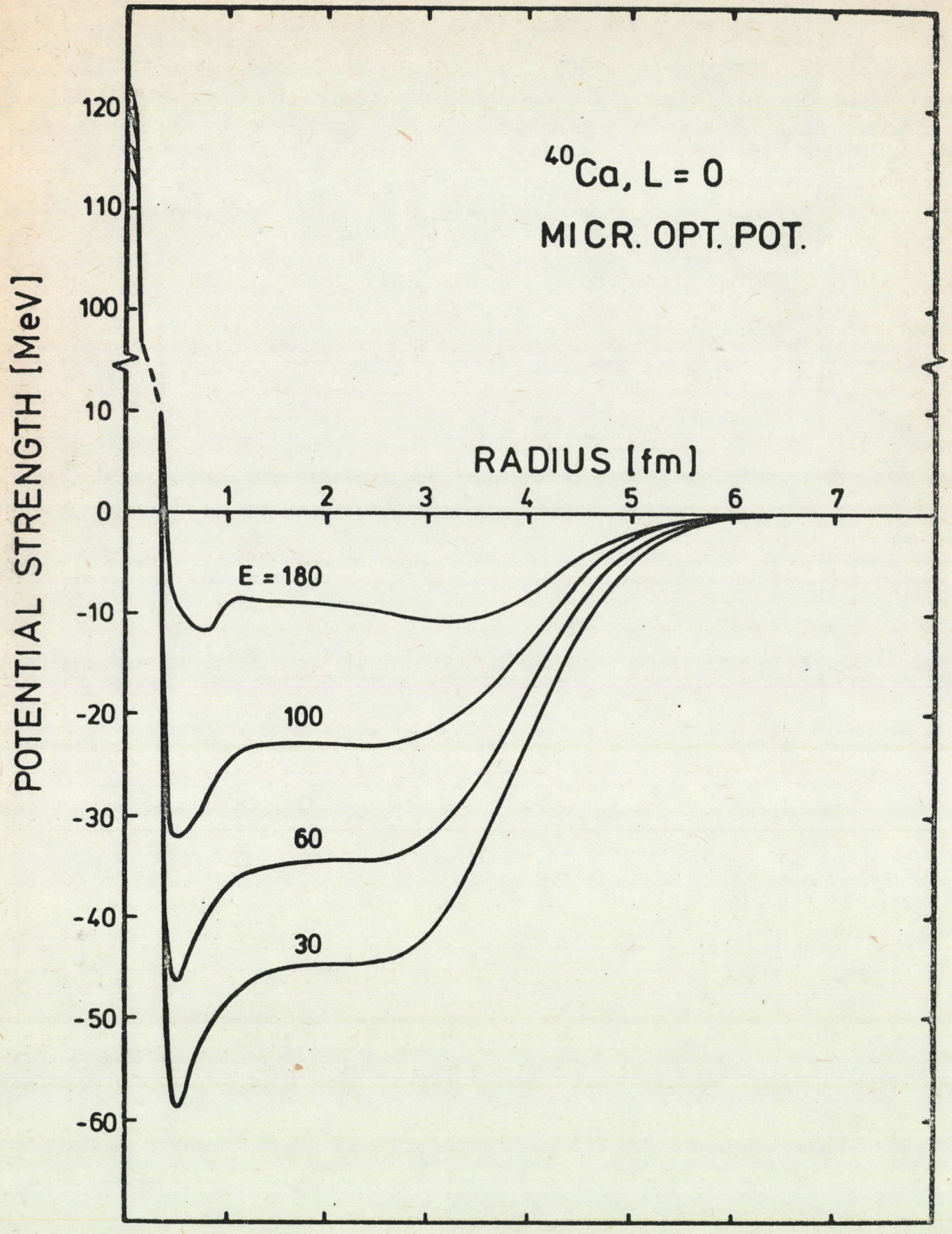
^{40}Ca, L = 0
MICR. OPT. POT.
RADIUS [fm]
POTENTIAL STRENGTH [MeV]
120
110
100
10
0
-10
-20
-30
-40
-50
-60
1
2
3
4
5
6
7
E = 180
100
60
30

FIG. 7

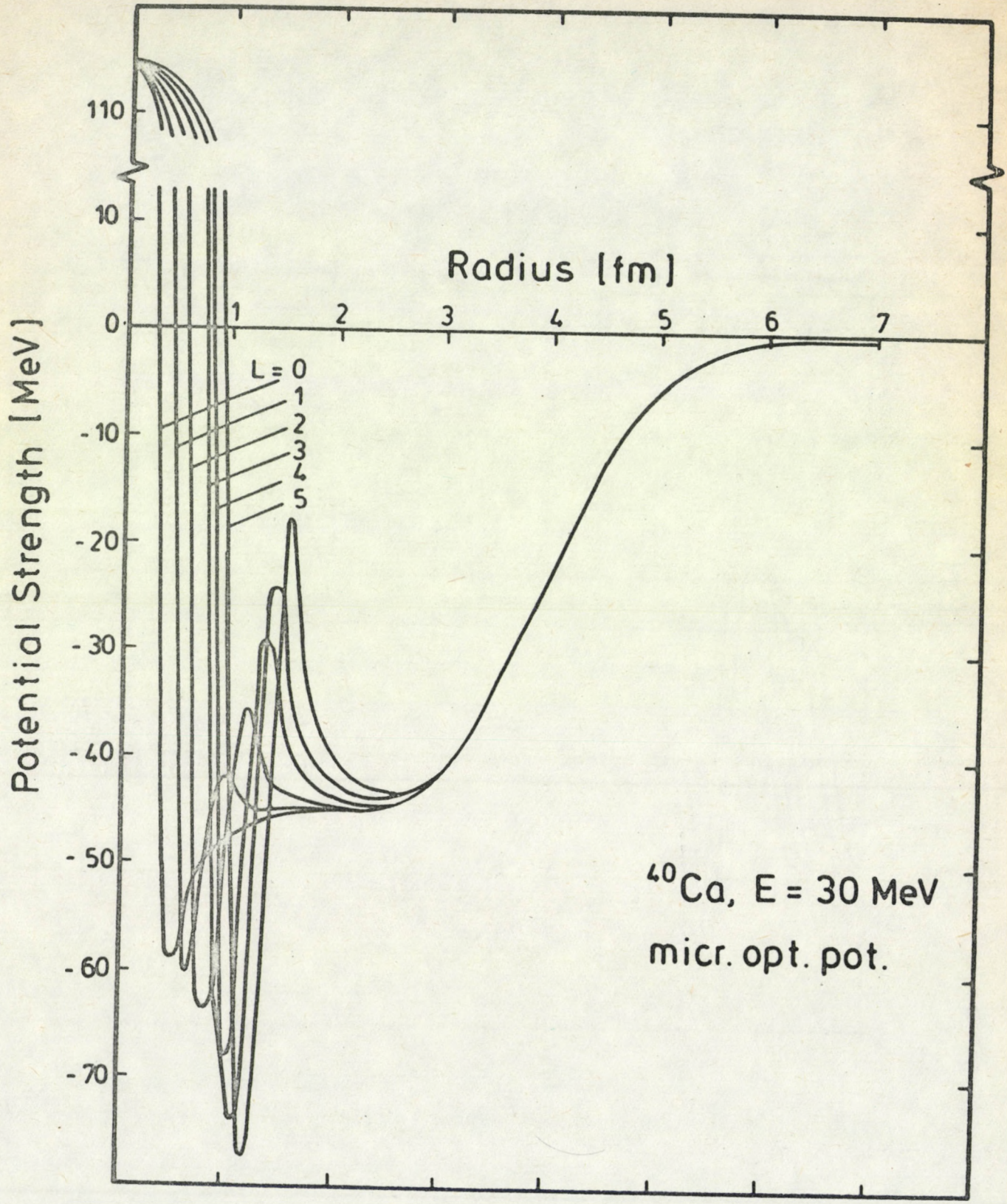
110
10
0
-10
-20
-30
-40
-50
-60
-70
Potential Strength [MeV]
Radius [fm]
1
2
3
4
5
6
7
L = 0
1
2
3
4
5
40Ca, E = 30 MeV
micr. opt. pot.

FIG. 8 A

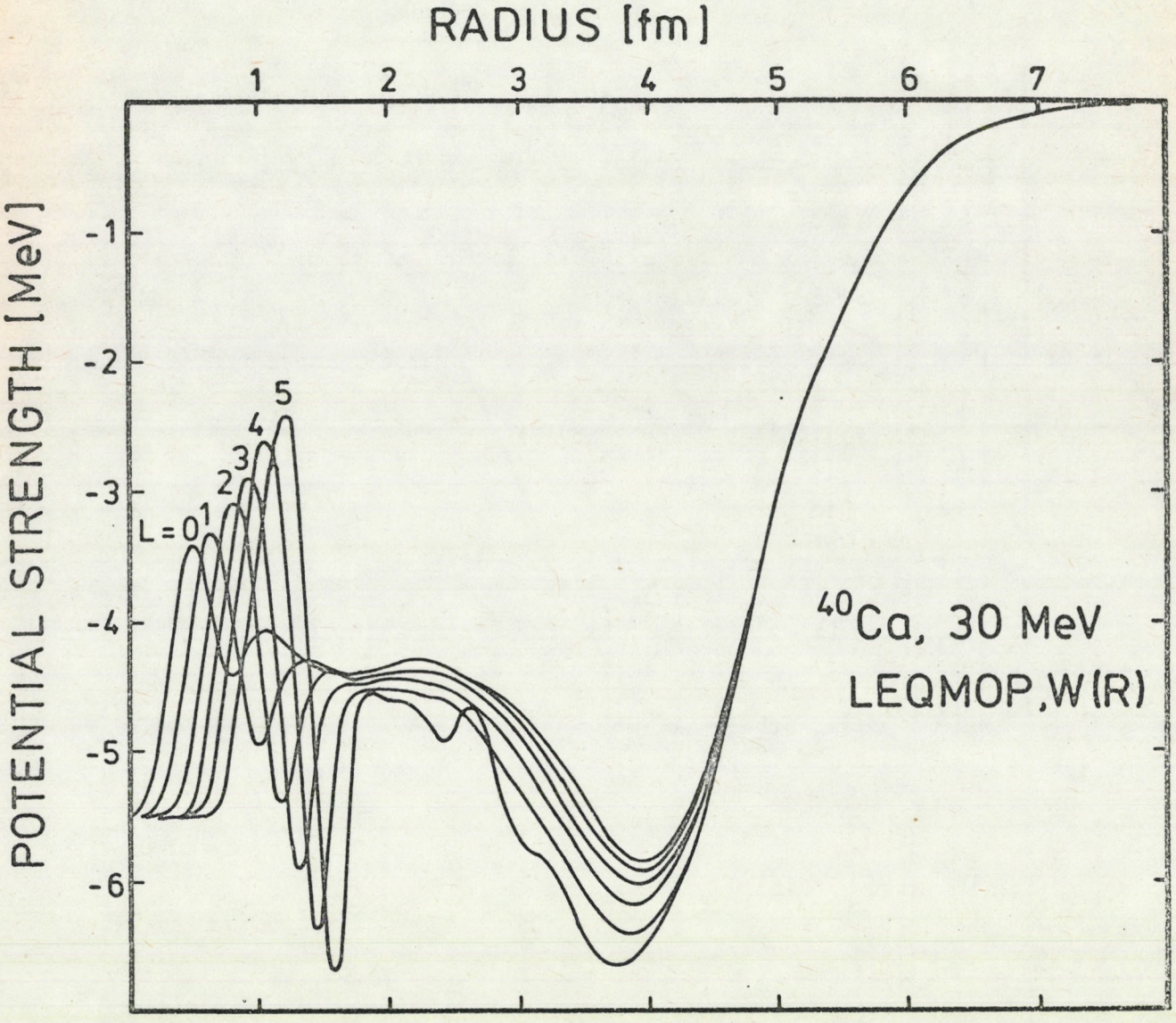
RADIUS [fm]
1
2
3
4
5
6
7
POTENTIAL STRENGTH [MeV]
-1
-2
-3
-4
-5
-6
L = 0
1
2
3
4
5
^{40}Ca, 30 MeV
LEQMOP, W(R)

FIG. 8 B

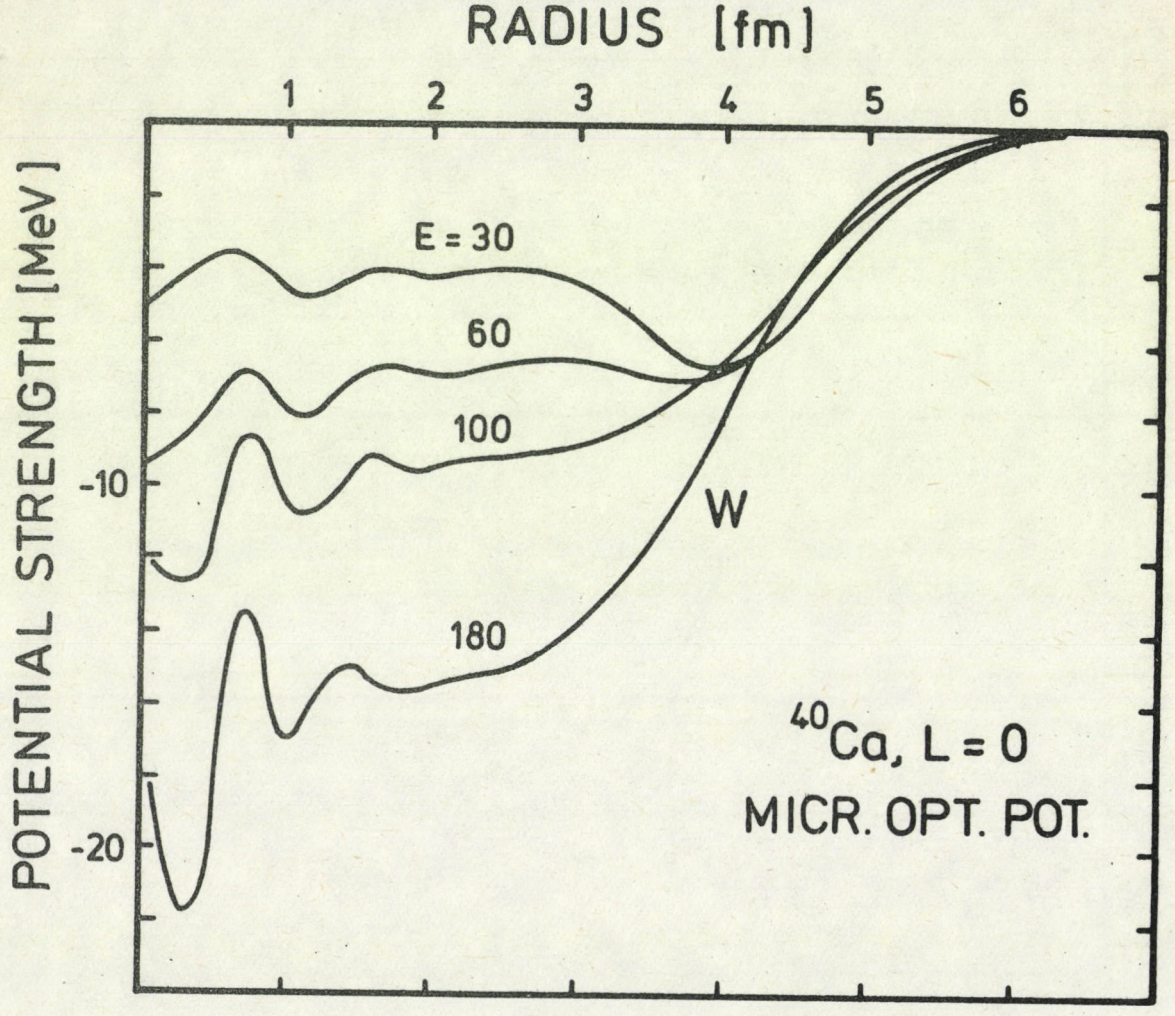
RADIUS [fm]
1
2
3
4
5
6
POTENTIAL STRENGTH [MeV]
-10
-20
E = 30
60
100
180
W
^{40}Ca, L = 0
MICR. OPT. POT.

FIG. 9 A

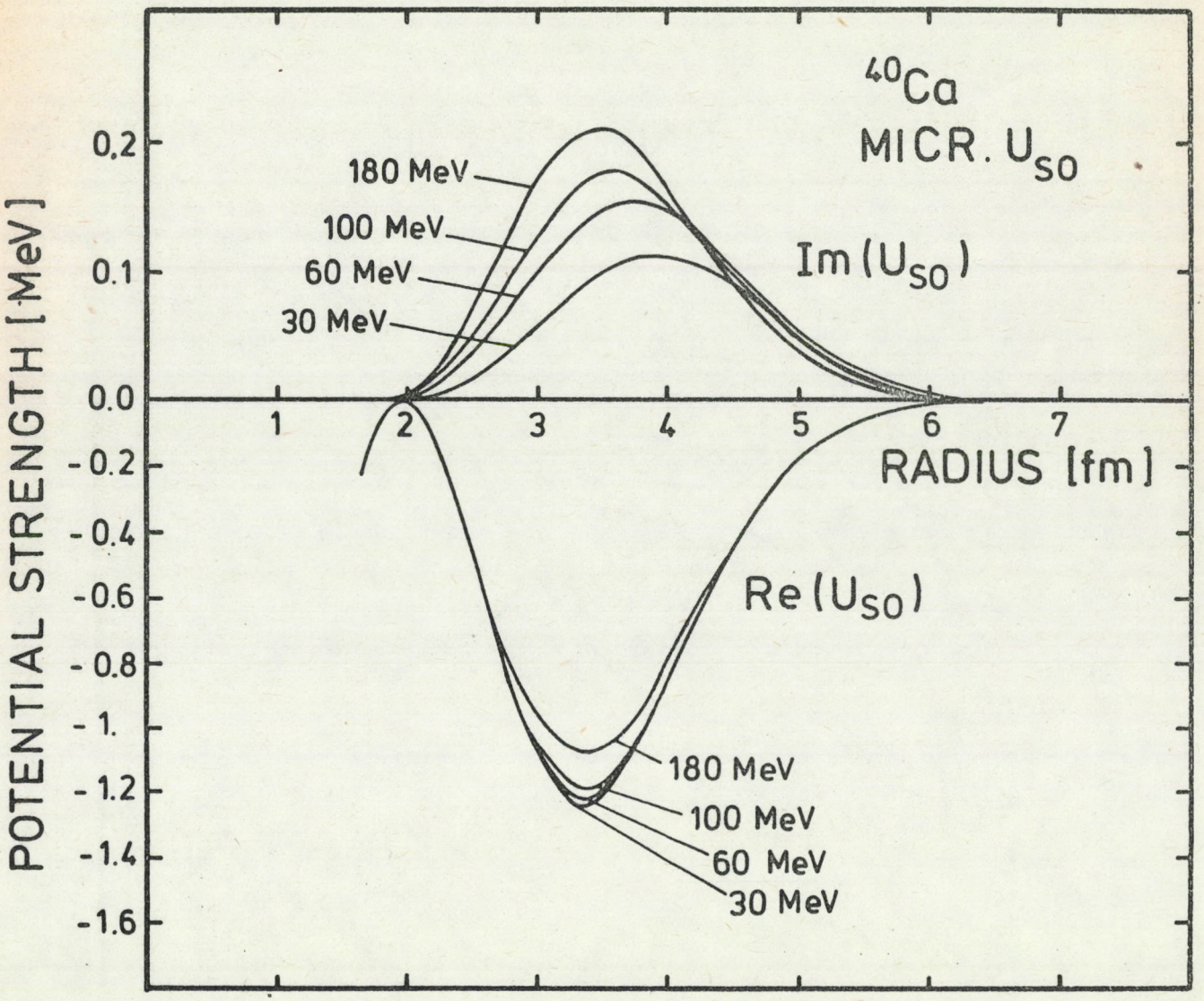
^{40}Ca
MICR. U_{SO}
Im (U_{SO})
Re (U_{SO})
180 MeV
100 MeV
60 MeV
30 MeV
180 MeV
100 MeV
60 MeV
30 MeV
POTENTIAL STRENGTH [MeV]
RADIUS [fm]
0.2
0.1
0.0
-0.2
-0.4
-0.6
-0.8
-1.
-1.2
-1.4
-1.6
1
2
3
4
5
6
7

FIG. 9 B

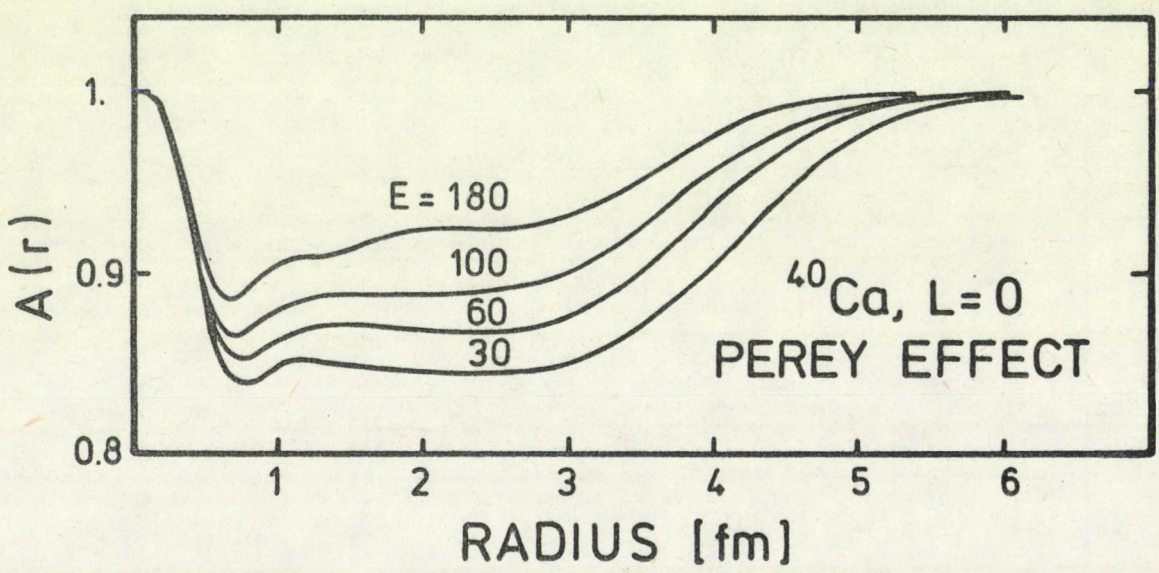

FIG. 9 c

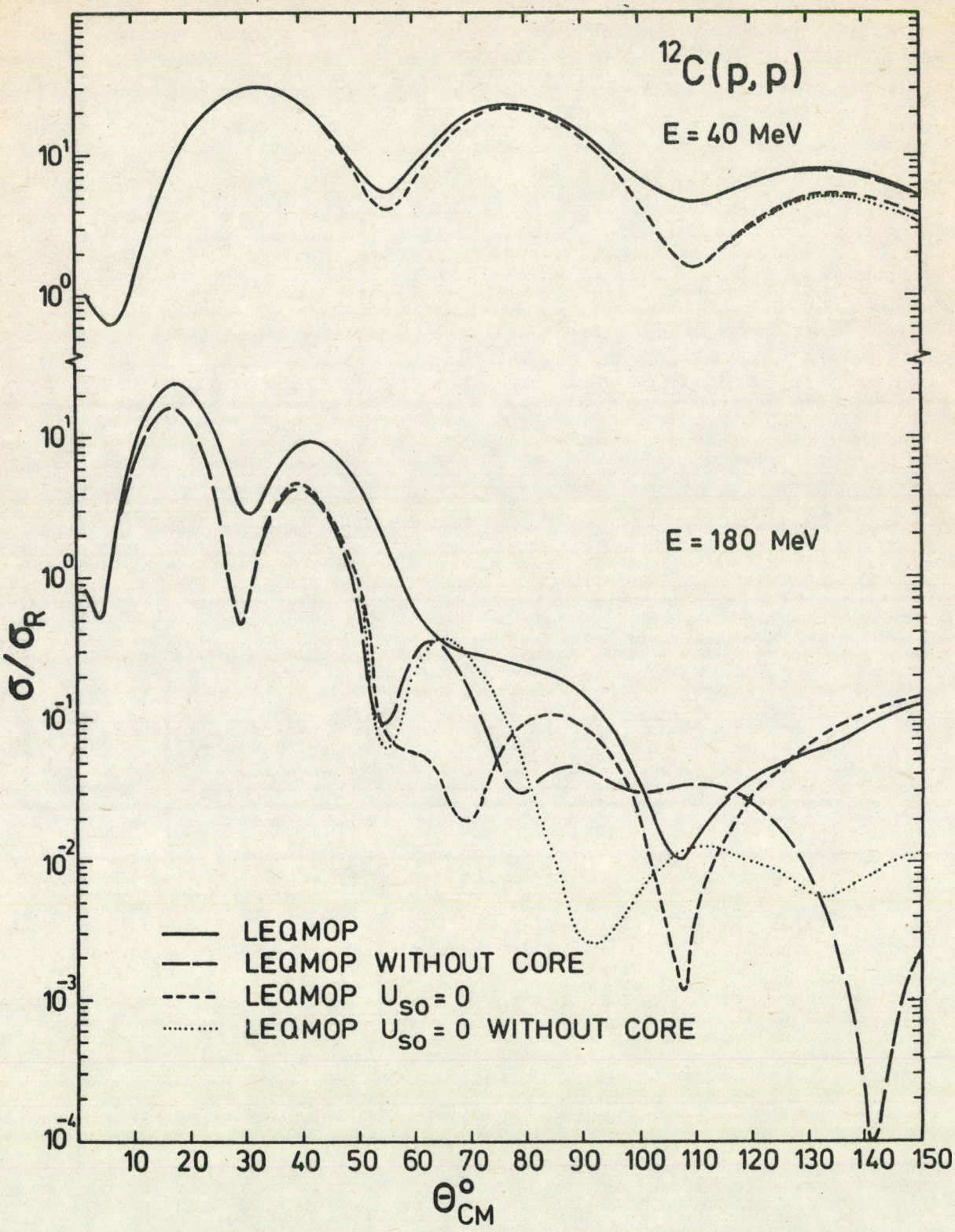
$^{12}C(p,p)$
E = 40 MeV
E = 180 MeV
σ/σ_R
θ°_{CM}
LEQMOP
LEQMOP WITHOUT CORE
LEQMOP $U_{so} = 0$
LEQMOP $U_{so} = 0$ WITHOUT CORE

FIG. 1o

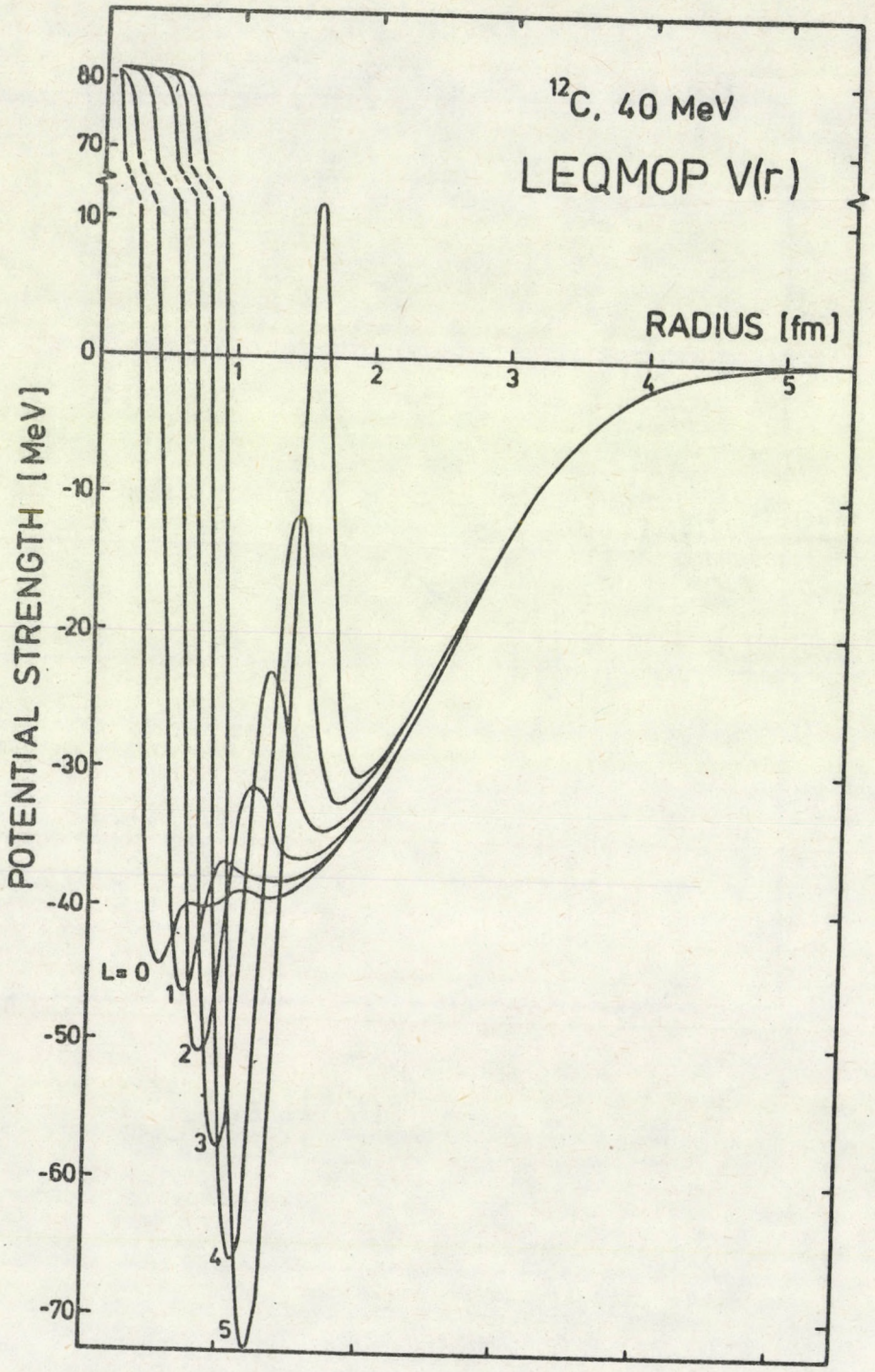
^{12}C, 40 MeV
LEQMOP V(r)
RADIUS [fm]
POTENTIAL STRENGTH [MeV]
80
70
10
0
-10
-20
-30
-40
-50
-60
-70
1
2
3
4
5
L= 0
1
2
3
4
5

FIG. 11 A

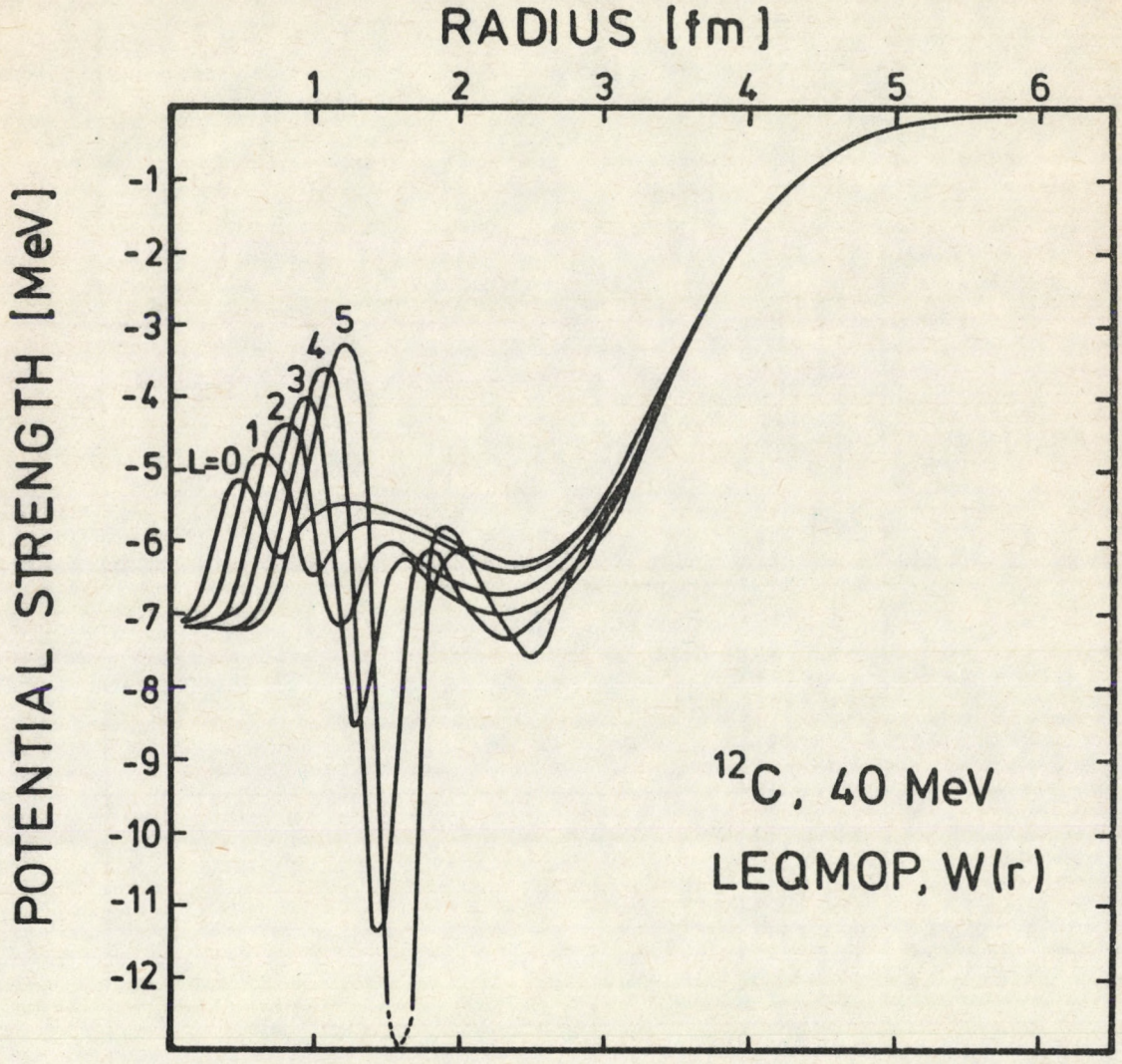
RADIUS [fm]
1
2
3
4
5
6
POTENTIAL STRENGTH [MeV]
-1
-2
-3
-4
-5
-6
-7
-8
-9
-10
-11
-12
L=0
1
2
3
4
5
^{12}C, 40 MeV
LEQMOP, W(r)

FIG. 11 B

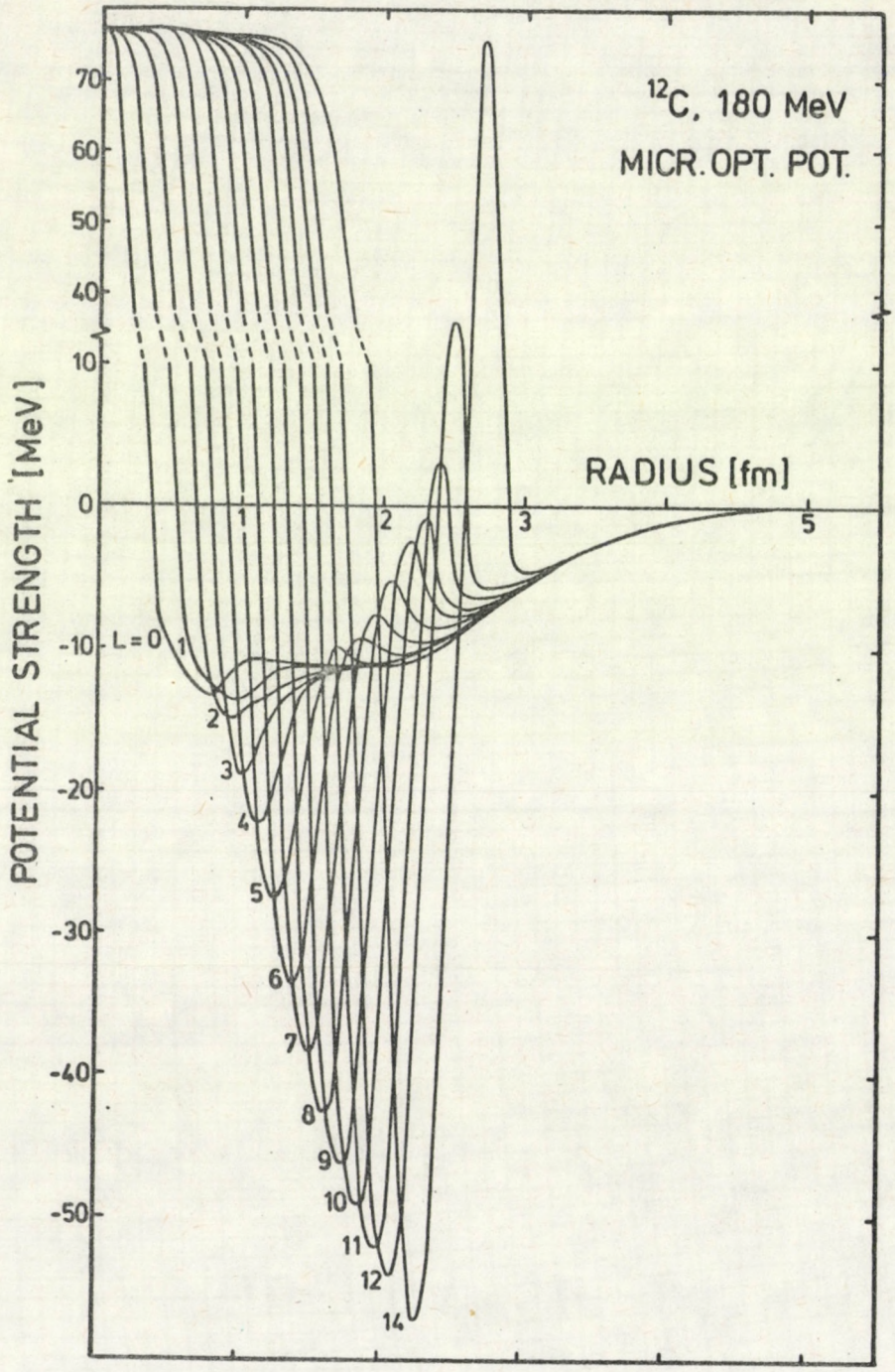
^{12}C, 180 MeV
MICR. OPT. POT.
RADIUS [fm]
POTENTIAL STRENGTH [MeV]
70
60
50
40
10
0
-10
-20
-30
-40
-50
1
2
3
5
L = 0
1
2
3
4
5
6
7
8
9
10
11
12
14

FIG. 12 A

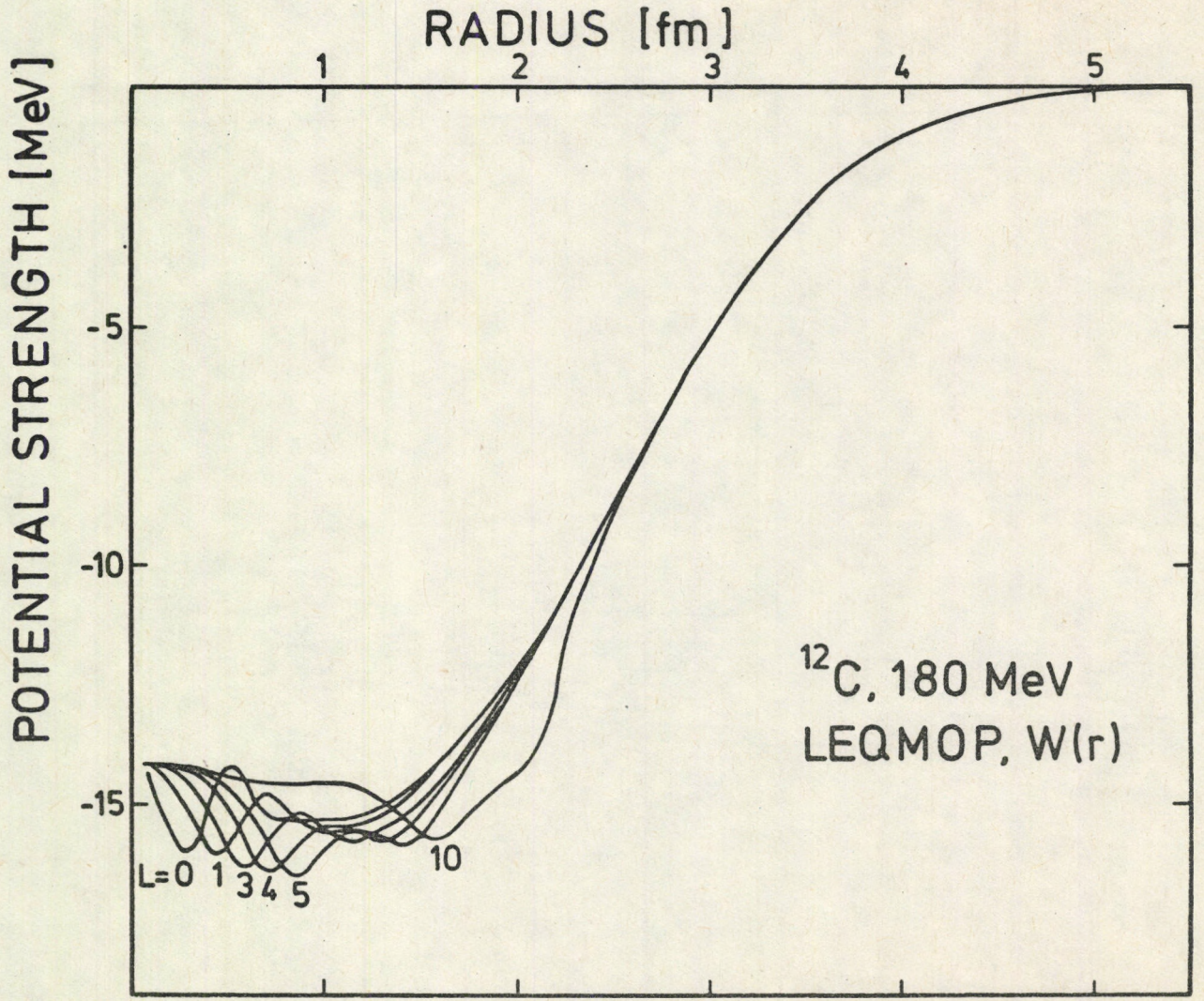
RADIUS [fm]
1
2
3
4
5
POTENTIAL STRENGTH [MeV]
-5
-10
-15
L=0 1 3 4 5
10
^{12}C, 180 MeV
LEQMOP, W(r)

FIG. 12 B

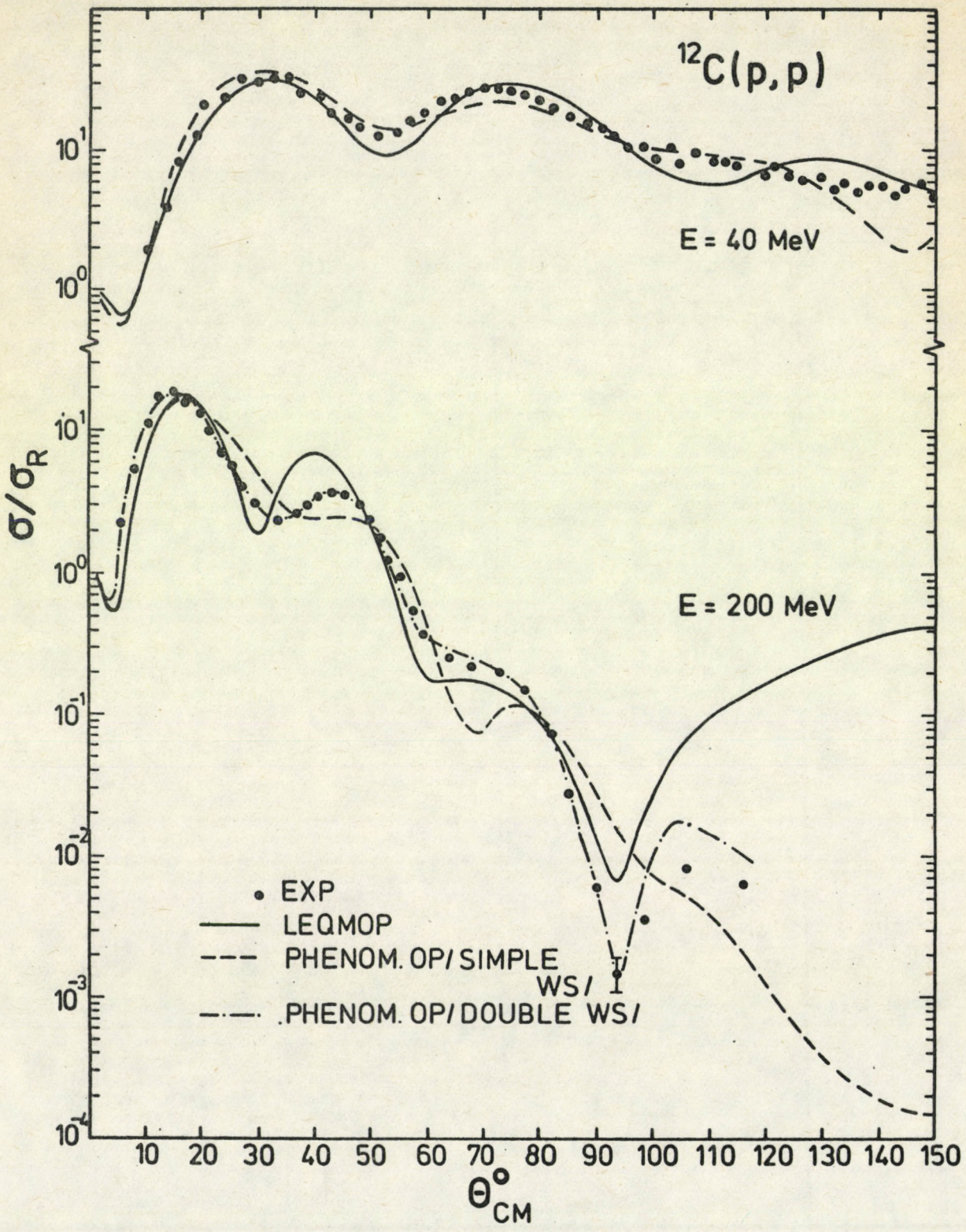
$^{12}C(p,p)$
E = 40 MeV
E = 200 MeV
σ/σ_R
θ°_{CM}
EXP
LEQMOP
PHENOM. OP/ SIMPLE WS/
PHENOM. OP/ DOUBLE WS/
10^{1}
10^{0}
10^{-1}
10^{-2}
10^{-3}
10^{-4}
10 20 30 40 50 60 70 80 90 100 110 120 130 140 150

FIG. 13

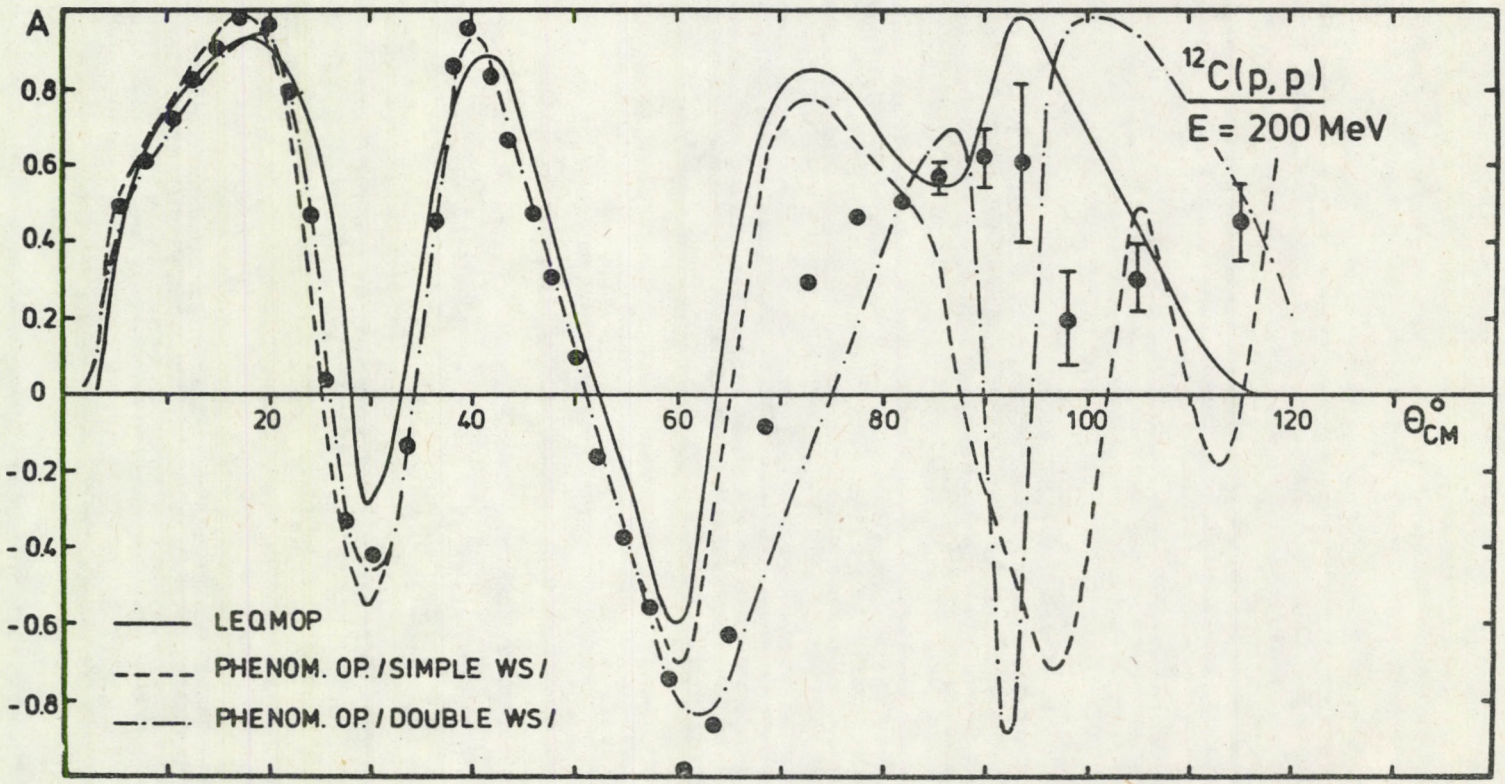
A
0.8
0.6
0.4
0.2
0
-0.2
-0.4
-0.6
-0.8
20
40
60
80
100
120
θ°_{CM}
$^{12}C(p,p)$
E = 200 MeV
LEQMOP
PHENOM. OP. / SIMPLE WS /
PHENOM. OP. / DOUBLE WS /

FIG. 14

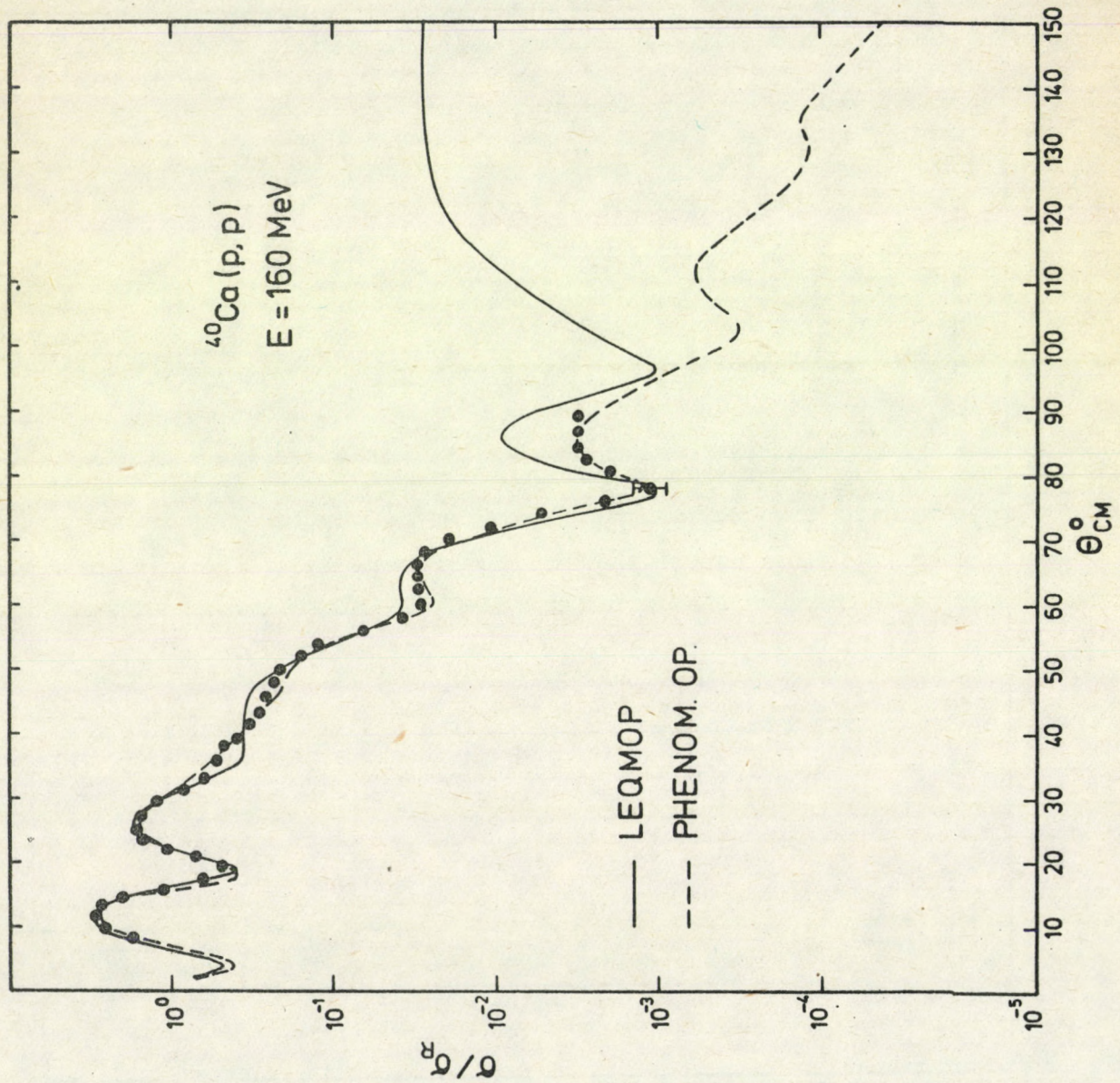
^{40}Ca (p, p)
E = 160 MeV
LEQMOP
PHENOM. OP.
σ/σ$_R$
θ°_{CM}
10^0
10^{-1}
10^{-2}
10^{-3}
10^{-4}
10^{-5}
10
20
30
40
50
60
70
80
90
100
110
120
130
140
150

FIG. 15 A

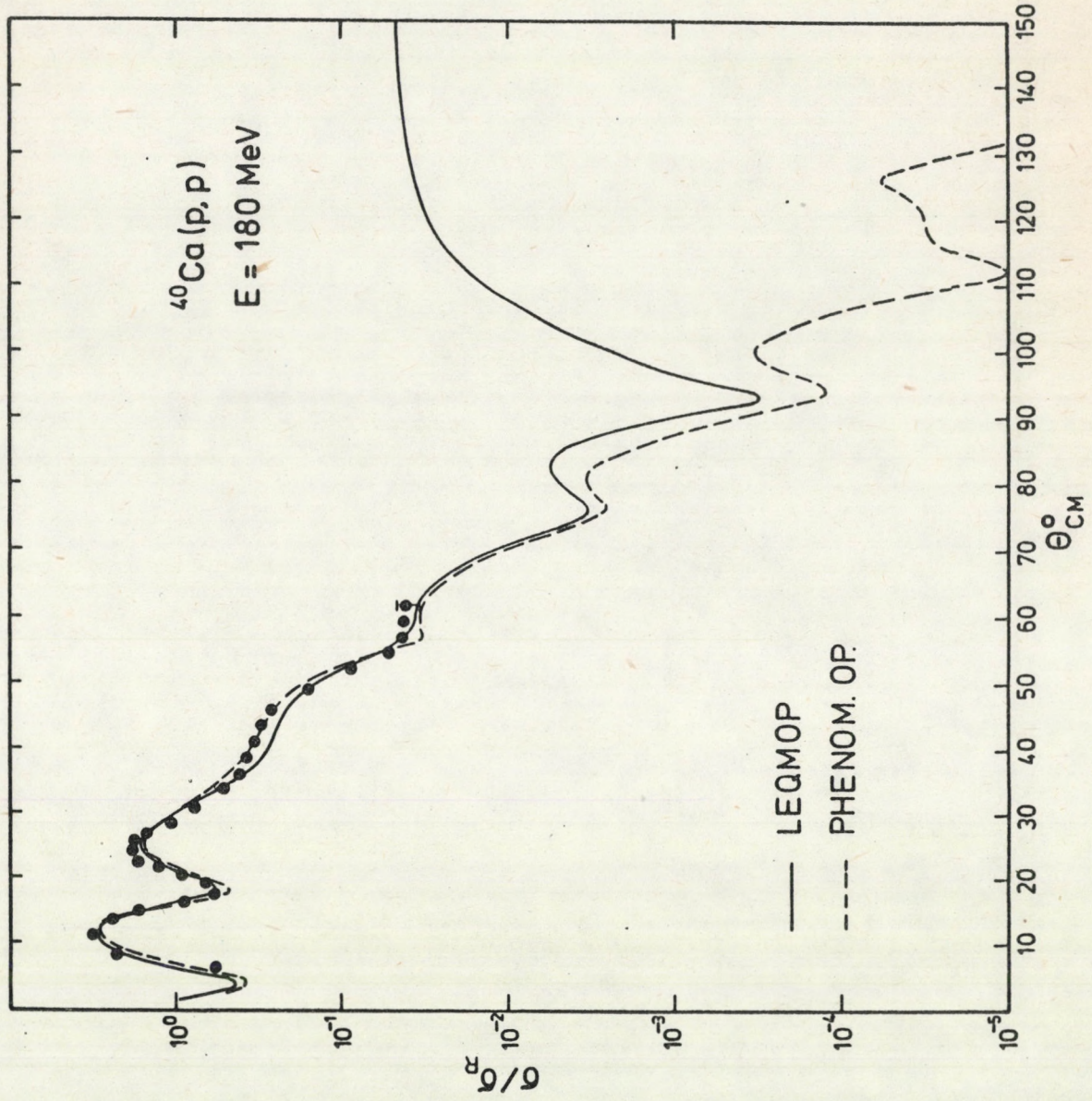
$^{40}Ca(p,p)$
E = 180 MeV
LEQMOP
PHENOM. OP.
σ/σ_R
θ°_{CM}
10^0
10^{-1}
10^{-2}
10^{-3}
10^{-4}
10^{-5}
10 20 30 40 50 60 70 80 90 100 110 120 130 140 150

FIG. 15 B

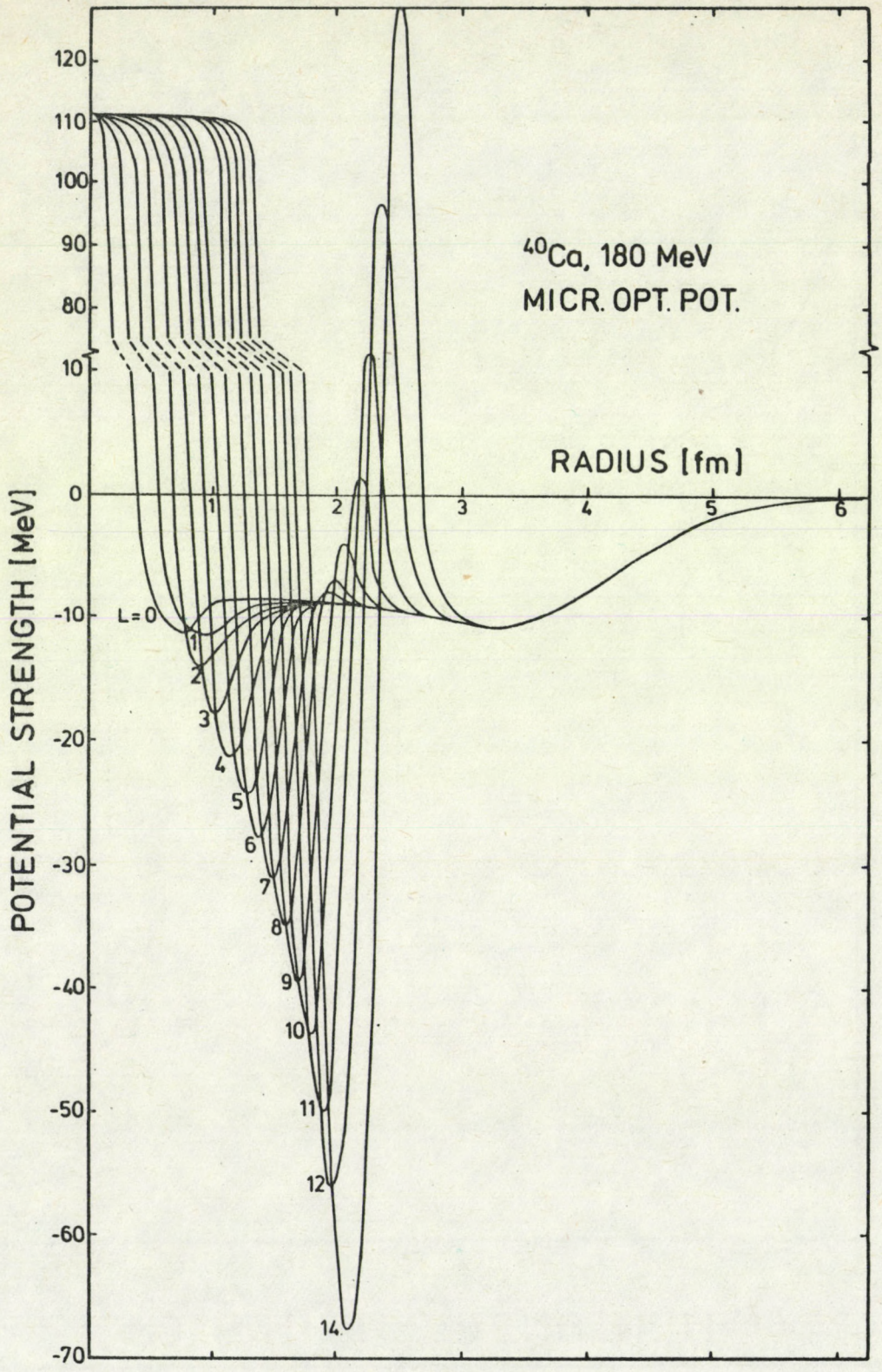
^{40}Ca, 180 MeV
MICR. OPT. POT.
RADIUS [fm]
POTENTIAL STRENGTH [MeV]
120
110
100
90
80
10
0
-10
-20
-30
-40
-50
-60
-70
1
2
3
4
5
6
L=0
1
2
3
4
5
6
7
8
9
10
11
12
14

FIG. 16 A

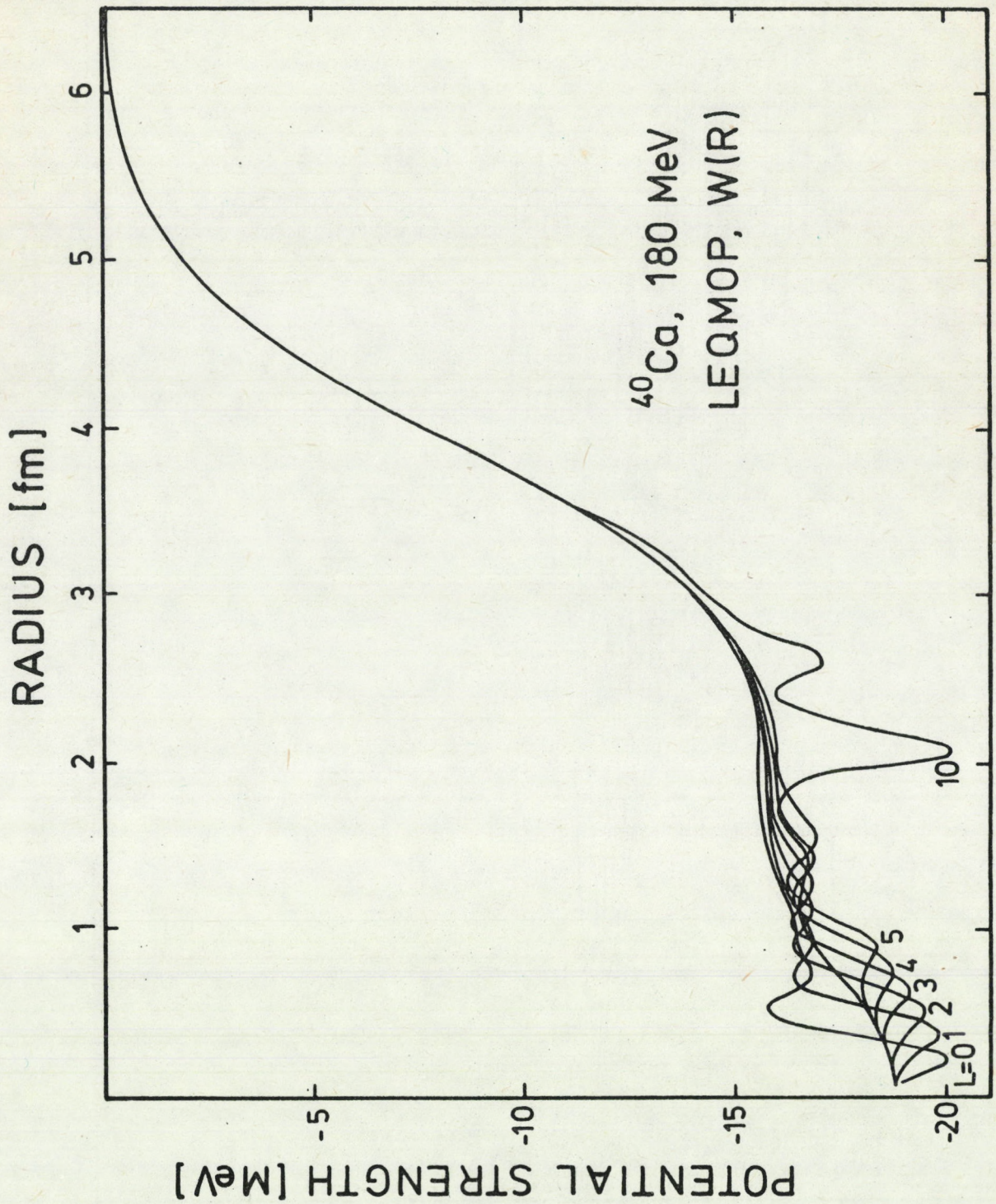
RADIUS [fm]
1
2
3
4
5
6
POTENTIAL STRENGTH [MeV]
-5
-10
-15
-20
^{40}Ca, 180 MeV
LEQMOP, W(R)
L=0
1
2
3
4
5
10

FIG. 16 B

63.107

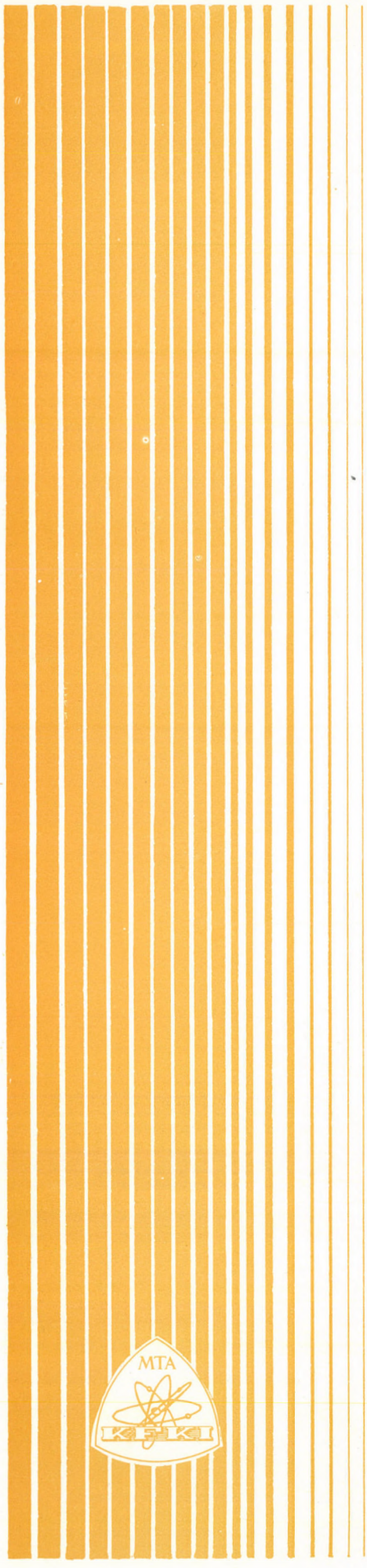

Kiadja a Központi Fizikai Kutató Intézet
Felelős kiadó: Szegő Károly
Szakmai lektor: Doleschall Pál
Nyelvi lektor: Kluge Gyula
Példányszám: 450 Törzsszám: 80-739
Készült a KFKI sokszorosító üzemében
Felelős vezető: Nagy Károly
Budapest, 1980. december hó